UNIVERSIDADE DE SÃO PAULO
INSTITUTO DE ASTRONOMIA, GEOFÍSICA E CIÊNCIAS ATMOSFÉRICAS
DEPARTAMENTO DE CIÊNCIAS ATMOSFÉRICAS

Interações Multi-Escala, Variabilidade de Baixa Frequência e o Aquecimento Global.

Julio Cesar Morais

TESE APRESENTADA AO INSTITUTO DE ASTRONOMIA,
GEOFÍSICA E CIÊNCIAS ATMOSFÉRICAS
DA
UNIVERSIDADE DE SÃO PAULO
PARA A OBTENÇÃO DO TÍTULO DE

DOUTOR EM CIÊNCIAS

ÁREA: METEOROLOGIA

Orientador: Prof. Dr. Carlos Frederico Mendonça Raupp

SÃO PAULO

(2020)

Versão Corrigida. O original encontra-se disponível na Unidade.

AGRADECIMENTOS:

Aos meus pais, Marco Antônio e Luzi, pelo amor, apoio e carinho demonstrados ao longo da minha vida que tornaram possível toda a caminhada até aqui. Por sempre acreditarem em mim e darem suporte a todas as minhas decisões. Pela dedicação em minha formação e sempre insistirem em valorizar a educação.

Ao professor Carlos Raupp: pela paixão e leveza com que discute os mais complexos temas. Pela gentileza, companherismo e respeito no relacionamento com os alunos e por todo conhecimento transmitido durante o doutorado, além de muito papo descontraído. Obrigado pela ajuda.

À Amanda de Paula, pelo amor demonstrado em palavras e ações nestes anos de relacionamento, pelo apoio e suporte em horas difíceis e por todos os momentos de alegria que, sem dúvida alguma, tornaram essa caminhada muito mais leve de ser percorrida.

À toda minha família, especialmente minha madrinha Regina, por todo apoio e incentivo ao longo desse anos sem os quais não poderia ter chegado até este ponto.

Ao meu sogro, Gilberto, e sogra, Ivanilda, por terem me recebido em sua família e demonstrado carinho e apoio desde o primeiro dia. Para toda a família fica meu especial agradecimento.

Aos amigos de sempre, de ontem e de hoje, por estarem presentes em minha vida e ajudarem de todas as maneiras possíveis. Estendo especial agradecimento ao André Teruya pelas discussões muito produtivas e pela paciência na ajuda com as simulações numéricas da tese.

Aos professores e funcionários do IAG-USP, pelas conversas e ajudas em todos meus anos de IAG.

Ao CNPQ e à CAPES, pelo financiamento dessa pesquisa.

CONTENTS

Abstract

The potential of the Madden-Julian Oscillation (MJO) to influence the climate and weather in both tropical and extratropical regions is of utmost importance for the global warming and climate change discussion. In this context, understanding how the MJO responds to the warming of the planet is a necessary step to build our physical comprehension on the way in which global warming influences extreme events of precipitation and temperature fields. Here we address the issue of the MJO response to global warming by means of a toy model of the MJO activity based on a single nonlinear triad interaction involving two convectively coupled equatorial wave modes, namely a Rossby and a Kelvin wave, and a barotropic Rossby mode. The two equatorial modes are known to play an important role in the planetary-scale circulation features associated with the MJO within the tropics, while the barotropic Rossby mode is related to its tropical-extratropical teleconnection. In addition, since moisture convergence is also known to play an important role in the MJO dynamics, here we mimic this effect by representing the coupling between the equatorial waves and moist convection in terms of the wave-CISK formulation. We also analyze in this formulation the role of the diurnal cycle of the moisture field, which can resonantly couple the equatorial Rossby mode of the triad with a high-frequency inertio-gravity wave. The inertio-gravity mode is thought of as representing the high-frequency convective systems embedded in the MJO. The effect of global warming is analyzed by changing the maximum value of the moisture field.

The results show that an enhanced moisture can allow the equatorial wave modes to get in resonance with the barotropic Rossby mode, making the wave triad to undergo stronger energy modulations. This stronger energy modulation of the triad interaction might suggest a stronger MJO activity under a moister (warmer) environment. Also, our results indicate that an increased moisture content renders possible the MJO low frequency envelope to excite a high frequency gravity mode. We further show by changing the amplitude of gravity mode that the energy modulation of the triad becomes more intense, with an enhanced back and forth energy transfer between the equatorial gravity and Rossby modes, affecting also the kelvin wave. This indicates a strong necessity of a better representation of gravity waves in GCMs in order to properly simulate the effect of global warming on the MJO.

List of figures

Figure 9: Phase space perspective of the integration displayed in Fig. 7, displaying the energy of Kelvin mode as a function if the ER mode energy

Figure 10: Similar to Fig. 7, but for another set of modes (see text) and for a diurnal cycle of the heat forcing being described by a half rectified sine function**.**

1 Chapter 1: INTRODUCTION

1.1 Global warming:

Climate change science has a somewhat illustrious past dating back at least to the beginning of the XIXth century. Joseph Fourier (1768 - 1830) and John Tyndall (1820 – 1893) already hiphotesized the idea that some of its constituting gases turns the atmosphere opaque for terrestrial radiation, what is known today as greenhouse effect in which some gases retain inside the Earth system part of infrared radiation that otherwise would be lost to space. Svant Arrhenius (1859 – 1927) was the first to associate the doubling in CO2 levels with a 4-degree increase in the global average temperature. An important step toward what is known as climate change science nowadays was Jules Charney´s report entitled: "Carbon dioxid and climate: a scientific assessment" from 1979. Again, the doubling of CO2 concentration in the atmosphere is associated with a rise in global temperature between 3 to 5 degrees. For a brief history of climate change science, see Neelin (2011, chapter 1.4.3) and Held and Soben (2000, chapter 1). However, it was not until the end of the XXth century that a systematic coherent approach to the climate change problem, the Intergovernmental Pannel of Climate Change (IPCC), begun under UN oversight.

The warming of the planet is one of the most clear aspects of the climate changes due to the steady increase of carbon dioxid concentration in the atmosphere. Furthermore, projections show that the concentration will rise further into the XXIst century, increasing the greenhouse effect associated with it (Le Quére et.al., 2014). An important consequence of the global temperature increase refers to its possible change on the extreme climate events, especially due to their economical and societal impacts (IPCC, 2013). In fact, observational studies have shown that both extreme heat waves and the heavy rainfall frequency and amplitude have increased in the last decades (Myhre et. al., 2019, Easterling et.al., 2000). In addition, modeling studies show that this increase of both amplitude and frequency of extreme climate events will continue further into the XXIst century (Seneviratne et al. 2012). Conversely, understanding how global warming influences the statistical properties of the climate variables, especially the tail of their probability distribution that defines the extreme climate events, is a rather difficult task. If the climate were a static thermodynamical system, the answer would rely only upon the increased capacity of the atmosphere to retain water vapor when undergoing warming, i.e, increasing the air temperature enhances the air capacity to retain water va-

por, which in turn increases rainfall on one hand and latent heat release on the other. However, the climate is a multiscale complex dynamical system in which the dynamics interacts with the thermodynamics in a simbiotic fashion. In this scenario, attributing to human activity the changing behaviour of hydrological cycle among other variables is no longer a trivial endeavour, as well as distinguishing the effects of the natural climate variability from those related to the antropogenic radiative forcing on the data (see, for instance, Compo and Sardeshmukh, 2010; Solomon et al. 2011).

Nevertheless, there are two major points that emerge from the IPCC report. The first point refers to the scientific basis of the attribution of the observed change in global climate (AR5, 2013), in which there is no doubt, despite of the difficulties mentioned above, that the recently observed warming of the planet is caused by the build up of greenhouse gases in the atmosphere related to human activity. The IPCC AR5 (2013) states that: "it is extremely likely that human influence has been the dominant cause of the observed warming since the mid twentieth century". The second point is regarding the uncertainty on the impact of the global warming on the whole climate system. In fact, there is a scientific gap to be fulfilled in order to correctly assess the properly representation of the principal climate variability modes in GCMs (General Circulation Models). The GCMs used in the IPCC simulations exhibit a not very accurately performance in representing even some of the most basic aspects of climate features (Flato et al. 2013), including cloud cover, convection organization and its interaction with large-scale dynamics and tropical-extratropical interactions (Wang et al. 2019). Bony et. al.(2015) argues for four urgent aspects, including the large-scale dynamics interaction with clouds, to be improved in future climate simulations for a better assessment of the effects of climate change. In spite of several improvements in the last decades, IPCC models still struggle to accurately simulate key aspects of climate dynamics. While this remains true, there will doubt cast on the assessment of climate change effects (Knutti, 2008).

In order for a numerical model of the climate system to accurately simulate it, it is necessary a better understanding of the physical mechanisms underlying the behaviour of the system and how a rise in the mean temperature field can affect these mechanisms. Generally, atmospheric processess are too complex and, consequently, it is commom the use of simplified theoretical models, or toy models, to analyse the dynamics of their evolution, limiting cases and their dependence upon key parameters. For example, Dijkstra, (2013) presented a series of toy models to describe some of the principal components of climate variability, such

as the North Atlantic Oscillation (NAO – Chapter 7) and the ElNiño (Chapter 8). Majda (2009) shows a toy model for the intraseazonal oscillation known as Madden-Julian Oscillation (MJO) that captures some of the main properties associated with this phenomenon. The aim of this work is to use a toy model of the MJO, following Majda (2009), to evaluate and assess the climate system response under the warming of the planet.

The MJO is the natural candidate to serving as a bridge between global warming and climate changes, especially changes in extreme events associated with the hydrological cycle such as floods and droughts, along with severe storms that in turn have enormous impact over human life and society. The IPCC models still struggle to accurately simulate the MJO (Jiang et al. 2015), what perhaps is one the most source of uncertainties for climate projections. Several modeling and observational studies have indicated a MJO activity change under climate change yet not conclusive (Jones and Carvalho, 2004; 2011; Arnold et al. 2013; Bui and Maloney, 2018; Rushley et al. 2019). That is the reason why a better conceptual understanding of the MJO is important, having been described as the "holy grail of tropical meteorology" (Raymond, 2001). This is a figure of speech employed by Raymond in order to highlight the extreme importance of the MJO and its effects on the whole climate and weather systems, which is the central to this work.

1.2 Madden-Julian Oscillation

The presence of the water vapor in the atmosphere, also called moisture, is a key characteristic of the tropical atmosphere. In the absence of horizontal temperature gradient, the amount of moisture is determinant for convection intensity (Sobel et al., 2001; Bretherton et al. 2004), a hypothesis that is known as weak temperature gradient (WTG). Tropical convection is organized into several time and spatial scales, from single cells to mesoscale systems (Houze, 2004), which build up the organization of synoptic-scale convectively coupled equatorial waves and ultimately the planetary-scale envelope of the MJO (Majda 2007; Kiladis et. al., 2009 and references therein).

The Madden Julian Oscillation (MJO) is the most prominent feature on intraseasonal (0-100 days) timescales in the tropical belt (Madden and Julian; 1971;1972). Not only does the MJO have a significant influence over tropical climate and weather, but it also affects the midlatitude circulation (Zhang, 2013; Lau and Waliser, 2012). One example of its importance

is the MJO influence over precipitation in the Amazon forest region (Muza and Carvalho 2006; Carvalho et al. 2008; Dias et al.2019) as well as in the SACZ (South Atlantic Converge Zone) (Carvalho et al. 2008; Muza et al. 2009; Grimm, 2019) that controls the amount of summertime precipitation in central and southeast Brazil, basically the major source of water for agriculture and energy productions of Brazil. In spite of its enormous importance for short-term climate variability, the MJO remains an important source of uncertainty for climate modeling. This uncertainty source in climate modeling by the MJO may be due to its lack of a deeper theoretical understanding. For a review of the state-of-the-art of the of theories that attempt to explain the MJO, see Wang et al.(2019).

The MJO is a global-scale envelope (10000-40000km) (wavenumber 1-4) of enhanced convection that appears in the Indian Ocean and propagates trough the western Pacific Ocean with a phase speed of the order of 5m/s (Madden and Julian, 1994) and group velocity close to zero (see Majda and Stechmann 2009 for the skeleton model of the MJO).

Therefore, due to its influence on the global climate, as well as its structure that naturally connects water vapor in the lower tropical atmosphere with the organized convection in mesoscale up to large-scale dynamics, the MJO is a natural candidate to serve as a bridge between global warming and climate change. This work rests strongly on the hypothesis that a possible way that global warming can alter global climate dynamics is via an increase in water vapor (moisture) concentration and latent heat release in convection processes. The effects of moist convection are twofold: it serves as the major source of energy in the tropical atmosphere through latent heat release and binds together large-scale dynamical features that comprise for the MJO envelope. Our focus here is to use the MJO as a conveyor belt linking warming of the planet and other global climate changes. The envelope of the MJO, in the most simplistic representation, can be viewed as a Matsuno-Gill (Matsuno , 1966 ; Gill, 1980) type of response to a heating in the midtroposphere, that is, an excitation of two equatorial wave types, equatorial Rossby and Kelvin waves having the first baroclinic mode vertical structure. In this simplified setting adopted here, the moisture spatio-variability couples these two equatorial wave-modes, resulting in the characteristic wave speed of the MJO-type feature. Apart from this tropical character of the MJO, another important characteristic feature of the MJO that makes it an obvious object of concern for any atmospheric scientist is its ability to influence weather and climate globally via its interaction with the major teleconnection patterns (Lau and Waliser, 2012). Indeed, the MJO interacts with the Pacific-North America

(PNA) pattern (Liebmann and Hartmann 1984), Pacific-South America pattern (PSA) (Mo and Higgins 1994), Antarctic oscillation (Carvalho et al. 2005) and the North-Atlantic Oscillation (NAO) (Lin et al. 2009; Jiang et al. 2017). The interaction of tropical modes of variability, such as the MJO, with middle and higher latitude circulations is another topic of extreme interest for theoretical analysis and has also been considered in this study.

1.3 Tropical-extratropical interaction:

The low-frequency variability (defined as time-scales longer than the synoptic-scale variability) of the atmospheric flow is characterized by the existence of significant anomalies of the dynamical fields having a highly coherent spatial variability. This coherent spatial structure makes the different geographically fixed centers of action of the climate anomalies to be strongly correlated with each other, characterizing the so-called teleconnection patterns. This concept was first introduced by Jacob Bjerknes while studying the El Niño impacts on the global climate and has been extensively applied in the contexts of climate modeling and observations. Some of these teleconnection patterns exhibit their action centers connecting tropical and extratropical regions, being therefore believed to be responsible for the connection between tropical and midlatitude circulations.

Besides the MJO being responsible for the dominant intraseasonal variability within the tropics, it also interacts with the midlatitude circulation via some of the teleconnection patterns mentioned above. For a complete review of teleconnections in the intraseasonal timescale involving the MJO, see Roundy (2012) and Stan et al. (2017). Observational evidences (e.g., Horel and Wallace1981; Wallace and Gutzler 1981; Blackmon et al. 1984; Karoly 1989) have shown that the teleconnection patterns linking tropics and extratropics are characterized by an equivalent barotropic vertical structure. Likewise, modeling studies on the impact of tropical thermal forcings have demonstrated that the atmospheric circulation obtained as a response to the imposed diabatic forcing is baroclinic over the tropics and barotropic over middle and higher latitudes (e.g., Simmons 1980; Hoskins and Karoly 1981). The latter point has justified the utilization of the barotropic vorticity model with a prescribed divergence forcing mimicking the upper troposphere effect of tropical heat sources in explaining the observed teleconnection patterns linking tropics and extratropics (e.g., Hoskins at al. 1977; Grimm and Silva Dias 1995; Coelho et al. 2014). Nevertheless, as the diabatic heating associ-

ated with deep convection only directly excites equatorially trapped wave modes having a first baroclinic structure (e.g., Gill 1980; Matsuno, 1966; DeMaria 1985; Kasahara 1984), a more complete theoretical description of the impact of tropical deep convection heating on the midlatitude circulation must consider a coupling mechanism of barotropic Rossby waves with baroclinic equatorial wave-modes. Kasahara and Silva Dias (1986) have pointed out the role of the linear coupling among the different vertical modes through the vertical shear of the background flow. Majda and Biello (2003) demonstrated the role of nonlinear resonance between barotropic and equatorial baroclinic Rossby waves in the long-wave region of the zonal wavenumber spectrum, while Raupp et al.(2008) studied the dynamics of resonant triads involving barotropic Rossby modes and other equatorial wave-types in the primitive equations. The latter work was extended in Raupp and Silva Dias (2009) with the inclusion of a diurnally varying diabatic forcing, which resonantly excites equatorial inertia-gravity modes that may constitute resonant triads with a barotropic Rossby wave-mode having a large midlatitude extension.

Therefore, the nonlinear interaction involving equatorial wave modes excited by deep convection heating and barotropic Rossby modes is an essential dynamical mechanism for the tropics-midlatitude teleconnections. As the MJO is known to be strongly coupled with deep convection heating, the nonlinear coupling mentioned above might also be a possible way of accounting for the MJO impact on the extratropics through its interaction with teleconnection patterns. Chen et al.(2015) derived an asymptotic reduced model for the tropics-extratropics interaction involving the MJO. Their model consists of a nonlinear triad interaction involving convectively coupled equatorial Rossby or Kelvin mode, a MJO mode and a barotropic Rossby mode. The MJO mode in their theoretical model is defined according to the skeleton model of Majda and Stechmann (2009), in which the MJO is a planetary-scale envelope described by a combination of nondispersive Rossby and Kelvin wave packets forced by deep convection heating, which in turn is parameterized in terms of a wave-activity field that represents meso-scale convective systems embedded in the planetary-scale envelope and a moisture transport equation. Here, we adopt a similar yet simpler approach based on a nonlinear triad interaction involving equatorial Rossby and Kelvin modes, both coupled with deep convection heating, and a barotropic Rossby mode. Despite the proximity with Chen et al. (2015), Majda and Biello (2003) and Majda and Stechmann (2009), the present work distinguishes from them in both the dynamical setting and scope. For instance, Chen et al. (2015) use MJO

as a mode in a triad interaction, while the present work uses the triad interaction to undersand the MJO envelope response to global warming. In addition, the skeleton model proposed by Majda and Stechmann (2009) does not describe the wave triad interaction as a way to think the large-scale envelope, instead they use a prescribed function to represent the envelope and link it with Rossby and Kelvin modes through moisture source and sink terms. Our setting is to use the triad interacion among planetary-scale wave modes in order to understand the changing in the MJO internal dynamics as a response to global warming.

1.4 The model and objective:

Given the fact that the Madden-Julian Oscillation (MJO) is one of the natural candidates to connect the increase of global average temperature and climate changes, the present study aims to investigate from a theoretical point of view, in terms of the governing equations of the atmospheric dynamics, the potential impact of the increase of the global average temperature of the atmosphere on the dynamics of the MJO.

For this purpose, given the considerations described in the previous sections of this chapter, we consider a simplified description of the MJO dynamics based on a single interacting wave triad composed of planetary-scale convectively coupled equatorial Rossby and Kelvin modes and a barotropic Rossby mode. The coupling between the equatorial wave modes with deep convection heating is described here in the simplest possible setting by adopting the linear wave-cisk hypothesis (Hayashi 1970; Stevens and Lindzen 1978) in which the heating is proportional to the lower-troposphere moisture convergence produced by the waves, with the moisture field being prescribed to mimic the observed meridional structure of the specific humidity in the atmosphere. If the diurnal cycle of the moisture field is considered, the triad is coupled with a fourth wave-mode, an equatorial inertia-gravity mode, through the linear wave interaction mechanism between equatorial Rossby and inertia-gravity modes proposed by Raupp and Silva Dias (2010). The presence of the inertio-gravity mode in this case can be thought of as representing the smaller-scale convective motion embedded in the MJO.

Then, the effect of global warming is studied by changing the maximum value of the specific humidity, since the warmer the climate the higher the water vapor concentration in the atmosphere, according to the Clausis-Clayperon law. We have shown that the moisture intensity plays a crucial role in the energy exchanges among the interacting waves of the triad

through the modification of the linear eigenfrequencies of the equatorial wave modes and thus the mismatch among the eigenfrequencies of the triad components. Thus, the results have shown that increasing the water vapor concentration of the atmosphere might trigger nonlinear resonances that are absent otherwise, and consequently increase the intensity of intraseasonal oscillations. Also, the results have shown that the water vapor can binds one slow motion mode such as an equatorial Rossby wave with a high frequency mode such as a gravity wave, through coupling with the diurnal cycle of the specific humidity. This mechanism provides a way by which the resonant triad can excite the gravity mode. Gravity modes are known to play a crucial role in the geostrophic adjustment and in triggering deep convection. Conversely, this mechanism can also potentially make the gravity wave to modulate the energy exchange inside the triad involving the MJO modes, thus influencing the MJO activity.

Due to the complexity of the climate system and consequently of its supposed responses and feedbacks with changes of the global average temperature, the analysis performed here aims to understand the essential physics related to the effect of global warming on the MJO by considering a toy model that contains the essential ingredients of the nonlinearity and the interaction between moist convection and large-scale wave dynamics. In fact, the three-wave interaction equations constitute the simplest setting of the nonlinearity manifestation and appear in any wave system having quadratic nonlinearities. Consequently, nonlinear triad interactions are widely studied in several fields of science, such as nonlinear optics, plasma physics and geophysical fluids dynamics. For a complete set of applications and theory review, see Craik (1985). Lynch (2003) describes the dynamics of resonant Rossby wave triads in the barotropic quasi-geostrophic equations and highlights its similarity with a simple mechanical system: the swinging spring. Kartashova and L'yov (2007) proposed a theoretical model for the intraseasonal oscillations of the atmosphere based on a cluster of a few connected triads of barotropic Rossby waves.

The remainder of this work is organized as follows. Chapter 2 presents the theoretical introduction as well the model description. Chapter 3 presents the numerical solutions of the toy model and analysis of results. Chapter 4 presents the concluding remarks. Chapter 5 presents sugestions for future works.

2 Chapter 2: Theoretical Introduction

2.1 Mathematical prelude:

In this short section we will establish some common ground of definitions and notations. To avoid obscuring the goal of this work, these mathematical background concepts have not been presented in a rigourous fashion.

2.1.1 Fourier Analysis:

In a periodic domain it is common to use Fourier modes to analyse the dynamical evolution of the system in linear PDEs. Basically, it is assumed that the solution is a series of all possible Fourier modes in the following sense:

$$\Psi(x,t) = \sum_{k=-\infty}^{k=\infty} c_k e^{i(kx-\omega t)} \tag{2.1}$$

where c_k denodes the mode amplitude. Equation (2.1) means that the solution is given as a sum of oscillation modes in space as well as in time, where k, known as wavenumber, is the frequency of oscillations in space and ω is the temporal oscillation frequency. The relation between ω and k is known as dispersion relation.

2.1.2 Vector basis and inner product:

A subset of elements in a vector space is called a basis if any element in the vector space can be uniquely written as a series of the elements of the subset. Example: the functions $\{e^{ikx}\}_{k\in Z}$ form a basis of the $L^2_{[0,2\pi]}$ space, i.e the space of square integrable functions in $2\pi-$periodic domain.

An inner product is a measure of the angle between two vectors in the space. Another way to understand is that, the inner product mesures the strenght of the projection of one vector onto another. The inner product used throughout this work is of the form:

$$\langle f, g \rangle = \text{inner product of f with g} = \int_a^b f_1 g_1^* + f_2 g_2^* + f_3 g_3^* dx \tag{2.2}$$

where $f = [f_1 \quad f_2 \quad f_3]^T$ and $g = [g_1 \quad g_2 \quad g_3]^T$, with the superscript "T" meaning transposition operation and * the complex conjugate.

A basis is said to be orthonormal if, given any of its elements χ, φ, $\langle \chi, \varphi \rangle = 0$ and $\langle \chi, \chi \rangle = 1$.

2.1.3 Eigenvectors and eigenvalues:

An equation of the form: $\Xi\Psi = \alpha\Psi$, where Ξ is a linear operator acting on the vector Ψ and α is a complex number, is said to be an eigenvector/eigenvalue problem. Given two vectors on a linear space, χ, φ, the operator Ξ is called self-adjoint if $\langle \Xi\chi, \varphi \rangle = \langle \chi, \Xi\varphi \rangle$. In this case, all eigenvalues are real numbers and the eigenvectors form an orthogonal set. The operator is said skew-hermitian if $\langle \Xi\chi, \varphi \rangle = -\langle \chi, \Xi\varphi \rangle$ .In this case, if the operator is bounded, the eingenvalues are all pure imaginary numbers and the eigenvectors also form an orthogonal set. In the present model, this property has been demonstrated by Silva Dias et al. (1983) for the linear operator associated with the first baroclinic mode equations.

2.1.4 Notation:

Throughout this work, the following symbols/operators/characteristic values are assumed:

$V_H = (u, v)$ is the horizontal wind vector filed, with u and v indicating its zonal (west - east) and meridional (south – north) components, respectively;

$V_H^{\perp} = (-v, u)$;

W is the vertical velocity field;

f is the Coriolis parameter;

$\frac{df}{dy} = \beta = 2{,}2810^{-11} m^{-1}s^{-1}$ is the meridional gradient of planetary vorticity at the equator;

$g = 9.8 ms^{-2}$ is the gravity acceleration;

$div_H = \frac{\partial}{\partial x} + \frac{\partial}{\partial y}$ is the horizontal divergence;

θ is the potencial temperature and $\theta_0 \approx 300k$ corresponds to its reference value;

N = 0.01 s^{-1} is the Brunt-Vaisala frequency or the buoyancy frequency of oscillation, which is assumed here to be a constant;

$\Delta = \frac{\partial^2}{\partial x^2} + \frac{\partial^2}{\partial y^2}$ is the horizontal Laplacian operator;

$\frac{D}{Dt} = \frac{\partial}{\partial t} + u\frac{\partial}{\partial x} + v\frac{\partial}{\partial y} + w\frac{\partial}{\partial z}$ is the material derivative;

$C_P = 1006\frac{J}{kgK}$ is the heat capacity at constant pressure;

H = 16km is the height of troposphere;

L_V = 2.5 X 10^6 J/Kg is the latent heat of vaporization/condensation.

2.2 The model description:

Boyd (2018, Chapter 2) describes the validity of a number of approximations widely used in geophysical fluid dynamics. The approximations we use in this work on the full primitive Euler equations constitute the so-called hydrostatic Boussinesq equations , on the equatorial beta-plane with rigid lid vertical boundary conditions with W = 0 at z = 0 and z = H. It is well-known that the separation of variables of these equations into the vertical and horizontal-time varying structures, lead to a Shallow Water (SW) system for each vertical mode, with the vertical mode solutions satisfying a Sturm-Liouville problem (Valis, 2017, Majda 2003). Mathematically, the Euler equations with the assumptions mentioned above takes the form:

$$\frac{DV_H}{Dt} + \beta y V_H^{\perp} = -\nabla_H P$$
$$div_H V_H + W_Z = 0$$
$$\frac{D\theta}{Dt} + \frac{N^2\theta_0}{g}W = S_Q \qquad \text{(2.2.1 a,b,c,d)}$$
$$\frac{\partial P}{\partial z} = \frac{g\theta}{\theta_0}$$

(2.2.1 a) is the horizontal momentum equation; (2.2.1b) is continuity or mass conservation equation; (2.2.1 c) the thermodynamic or energy conservation, with S_Q denoting the

diabatic heat forcing; (2.2.1 d) is the hydrostatic balance equation and W_Z in equation (2.2.1b) refers to the vertical derivative of the vertical velocity.

The separation of variables mentioned above leads to an equation for the vertical structure of the form:

$$L\Theta_m = \lambda\Theta_m$$

where $L = \frac{d^2}{dz^2}$ and $\lambda = \frac{N^2}{c^2}$, with c being the separation constant. For the rigid-lid boundary conditions $\frac{d\Theta}{dz} = 0$ at z = 0 and z = H, the eigensolutions of this Sturm-Liouville problem are given by: $\Theta_m = \left\{\cos(\frac{m\pi z}{H})\right\}_{m=0,1,2...}$. Similarly, the separation constant c is obtained from the eigenvalues λ according to: $c_m = \frac{NH}{m\pi}$.

As the vertical structure equation with the rigid-lid boundary conditions constitute a Sturm-Liouville problem, the operator L is self-adjoint and the eigensolutions forms an orthogonal set.

The m=0 mode is called the barotropic mode, m=1 the first barocinic mode and so on. The field variables of equations (2.2.1) can then be written in the following way:

$$\begin{pmatrix} V_H(x,y,z,t) \\ P(x,y,z,t) \end{pmatrix} = \begin{pmatrix} V(x,y,t) \\ p(x,y,t) \end{pmatrix} + \begin{pmatrix} V_1(x,y,t) \\ p_1(x,y,t) \end{pmatrix} \sqrt{2}\cos(\frac{\pi z}{H})$$

$$\begin{pmatrix} W(x,y,z,t) \\ \Theta(x,y,z,t) \end{pmatrix} = \begin{pmatrix} w(x,y,t) \\ \theta(x,y,t) \end{pmatrix} \sqrt{2}\sin(\frac{\pi z}{H}) \qquad \text{(2.2.2 a,b,c)}$$

$$S_Q(x,y,z,t) = S_q(x,y,t)\frac{\pi}{2H}\sin(\frac{\pi z}{H})$$

where $\sqrt{2}$ is a suitable normalization constant. Equations (2.2.2 a,b, c) constitute the truncated Galerkin expansions retaining only the barotropic and the first baroclinic modes for the solution, as well as a single deep convection heating profile for the diabatic heat forcing. Such truncation was considered because we are interested only in the barotropic mode associated with tropical-extratropical interactions and the first baroclinic mode related to deep

convection heating. This truncation has been considered in both theoretical and modeling studies on the MJO (e.g., Fuchs and Raymond 2017). Majda and Stechmann (2003),; Khouder and Majda (2001), among others, include the second baroclinic mode related to shallow and stratiform clouds, which are necessary for a more accurate description of the MJO life cycle.

However, for simplicity we shall consider here only the deep convection heating and, therefore, truncation (2.2.2a, b, c) is sufficient.

Substituing (2.2.2) into (2.2.1), taking the z-derivative of (2.2.1c), using the continuity and hydrostatic balance equations into (2.2.1c) and taking the projection of (2.2.1) onto the barotropic and first baroclinic modes yield:

$$\frac{\partial \mathrm{V}}{\partial \mathrm{t}} + \mathrm{V} \bullet \nabla \mathrm{V} + \mathrm{V}_1 \bullet \nabla \mathrm{V}_1 + (\mathrm{div}_{\mathrm{H}} \mathrm{V}_1)\mathrm{V}_1 + \beta \mathrm{y} \mathrm{V} = -\nabla \mathrm{p};$$
$$\mathrm{div}_{\mathrm{H}} \mathrm{V} = 0;$$

(2.2.3 a,b,c,d)

$$\frac{\partial \mathrm{V}_1}{\partial \mathrm{t}} + \mathrm{V} \bullet \nabla \mathrm{V}_1 + \mathrm{V}_1 \bullet \nabla \mathrm{V} + \beta \mathrm{y} \mathrm{V}_1 = -\nabla \mathrm{p}_1;$$
$$\frac{\partial \mathrm{p}_1}{\partial \mathrm{t}} + \mathrm{V} \bullet \nabla \mathrm{p}_1 + \mathrm{c}^2 \mathrm{div}_{\mathrm{H}} \mathrm{V}_1 = -\mathrm{S}_{\mathrm{q}}.$$

where c is the separation constant associated with the first baroclinic mode, $c = c_1 = \frac{NH}{\pi}$ and $\bullet$ is the usual scalar product between two vectors in $\Re^3$. Physically, the parameter c represents the characteristic speed of the linear equatorial wave modes, as will be seen later. Equations (2.2.3 a,b) represent the evolution of the barotropic mode. The condition of nondivergence appears because the characteristic velocity of the baroropic mode , m=0, is infinite, which implies the nondivergent condition in order for finite solutions to be possible; S_q represents the projection of the vertical derivative of the diabatic heat forcing onto the first baroclinic mode vertical structure.

2.3 Solutions of the linearized and unforced system

Equations (2.2.3 a,b), when linearized around a resting state, take the form:

$$\frac{\partial \mathrm{V}}{\partial \mathrm{t}} + \beta \mathrm{yV} = -\nabla \mathrm{p}; \qquad \mathrm{divV} = 0\ . \tag{2.3.1 a,b}$$

Due to the nondivergence condition, (2.3.1) can be written in the streamfunction-vorticity version by taking the curl of equation (2.3.1a):

$$\frac{\partial \Delta\Psi}{\partial t} + \beta \frac{\partial \Psi}{\partial x} = 0 \tag{2.3.2}$$

where Ψ is the stream function given by $(u,v) = (-\Psi_y, \Psi_x)$ and $\Delta\Psi$ is the relative vorticity. Let us consider the following ansatz for equation (2.3.2):

$$\Psi(\mathrm{x},\mathrm{y},\mathrm{t}) = \mathrm{B}e^{\mathrm{i}(\mathrm{kx}-\omega \mathrm{t})} \sin(\mathrm{ly})$$

where the sine function is chosen for the meridional structure in order for the solution to have a zero meridional velocity at the meridional boundaries defined at $y = \pm L_y$, with L_y representing the distance from the equator to a pole. In fact, in a more realistic model that considers the compressibility of the atmosphere, the barotropic waves have a small decay factor multiplying the meridional eigenfunction (Raupp et al. 2008), so that the exactly non-trapping nature of the barotropic waves obtained here does not significantly differ from the divergent barotropic Rossby waves of the compressible primitive equations.
Substituing the above ansatz into (2.3.2), the following dispersion relation is obtained:

$$\omega(k) = -\frac{\beta k}{k^2 + l^2} \tag{2.3.3}$$

Equation (2.3.3) is the well-known dispersion relation of the barotropic Rossby waves. As one can easily verify, the barotropic Rossby wave is not equatorially trapped,

which makes it ideal for connecting the tropical region with the extratopics. In addition, it has been shown that the barotropic Rossby wave activity peaks at midlatitude regions, that is, if somehow a barotropic Rossby mode is excited at the equatorial region it will reach the maximum amplitude at midlatitudes. Details about the barotropic nondivergent equations can be found in Pedlosky (1987).

Assuming non-forced solutions, the equations (2.2.3 c,d), linearized about a resting state take the following form:

$$\frac{\partial V_1}{\partial t} + \beta y V_1 = -\nabla p_1$$
$$\frac{\partial p_1}{\partial t} + c^2 div V_1 = 0$$

or, alternatively, in non-vectorial form:

$$\frac{\partial u_1}{\partial t} - \beta y v_1 = -\frac{\partial p_1}{\partial x};$$
$$\frac{\partial v_1}{\partial t} + \beta y u_1 = -\frac{\partial p_1}{\partial y}; \qquad (2.3.4\ a,b,c)$$
$$\frac{\partial p_1}{\partial t} + c^2 div V_1 = 0.$$

The system above is the well-known shallow water (SW) system. For details of SW theory, including laws of conservations, see (Zeitlin, 2018). Also, for a more thorough description of the solutions and mathematical properties of (2.3.3) system, see (Majda, 2003 Chapter. 9). Matsuno (1966) was the first to derive the solutions of equations (2.3.3) as zonally propagating waves (Pedlosky 1987; Vallis, 2017) In summary, following Matsuno (1966), one seeks wave solutions as in (2.1):

$$I(x,y,t) = \sum_{k=-\infty}^{k=\infty} c_k(y) e^{i(kx-\omega t)} \qquad (2.3.5)$$

where $I(x,y,t) = [u(x,y,t) \quad v(x,y,t) \quad p(x,y,t)]^T$ and $c_k(y) = [\hat{u}(y) \quad \hat{v}(y) \quad \hat{p}(y)]^T$ represents the wave the amplitudes. The amplitudes have a functional dependance on the y-direction allowing the wave activity to either increase or decrease away from the equator. Physically, the

waves must decay far away from the source, and, this can only happen if the amplitude decays away from equator, that is, the solutions be equatorially trapped. In this sense, the equator here acts as a waveguide in which a myriad of wave types exists. Contrary to midlatitudes where the size of the Coriolis parameter f constrains the large-scale movement to be approximately geostrophic, in the equatorial belt the Coriolis parameter is small and changes its sign, allowing for other types of large-scale wave motions to coexist. Substituing (2.3.5) into (2.3.4), the following matrix system is obtained:

$$-i\omega\Theta + L\Theta = 0\,; \quad L = \begin{pmatrix} 0 & -\beta y & ik \\ \beta y & 0 & \dfrac{\partial}{\partial y} \\ ik & \dfrac{\partial}{\partial y} & 0 \end{pmatrix} \tag{2.3.6}$$

As one can easily verify the linear operator above is skew-hermitian, which implies that the eigenvalues $i\omega$ are pure imaginary, meaning the temporal frequency ω is a real value, thus there is no source of instability in this setup. Also, the fact that the linear operator L in (2.3.6) is skew-hermitian implies that the corresponding eigenvectors form an orthogonal set regarding the inner product defied in (2.2) with the interval [a, b] being replaced by $]-\infty \quad \infty[$.

After properly algebraic manipulations, it is possible to reduce the system (2.3.6) to a single differential equation for the meridional wind:

$$\frac{d^2v}{dy^2} + \left(\frac{\omega^2}{c^2} - k^2 - \frac{\beta k}{\omega} - \frac{\beta^2 y^2}{c^2}\right)v = 0 \tag{2.3.7}$$

This is the well-known quantum harmonic oscillator whose solutions are described in Quantum Physics textbooks. Equation (2.3.7) admits bounded solutions only if:

$$\frac{c}{\beta}\left(\frac{\omega^2}{c^2} - k^2 - \frac{\beta k}{\omega}\right) = 2n+1 \tag{2.3.8}$$

where n is a positive integer, called meridional wavenumber. Two fundamental constants appear in the equation above: c and β. These constants are used to make (2.3.8) dimensionless in the following fashion:

$$\omega \to \frac{\omega}{(\beta c)^{\frac{1}{2}}}, y \to y(\frac{\beta}{c})^{\frac{1}{2}}; k \to k(\frac{c}{\beta})^{\frac{1}{2}} \tag{2.3.9}$$

Thus, equation (2.3.8) in nondimensional form is written as:

$$(\omega^2 - k^2 - \frac{k}{\omega}) = 2n+1 \tag{2.3.10}$$

This cubic equation above defines the dispersion relation for the linear wave solutions of the first baroclinic equations. There are three distinct roots of (2.3.10) corresponding to slow motion equatorial Rossby waves (ER) and two fast modes corresponding to an eastward inertia-gravity wave and a westward inertia-gravity wave. An especial case refers to n = 0, where there are only two branches. One branch represents a slow westward propagating mode that is similar to the slow Rossby modes for large zonal wavenumbers and to the inertio-gravity modes for small zonal wavenumbers. The other one is an eastward propagating inertio-gravity mode. The westward branch of the n = 0 solution has been labeled as mixed Rossby-gravity mode or Yanai mode. There is yet another solution not contemplated by (2.3.7). This solution appears when the meridional wind is set zero and is called Kelvin wave, being labelled as n=-1 for completeness. Fig.1 shows all the eigenmodes of the linearized first baroclinic equations (2.3.4).

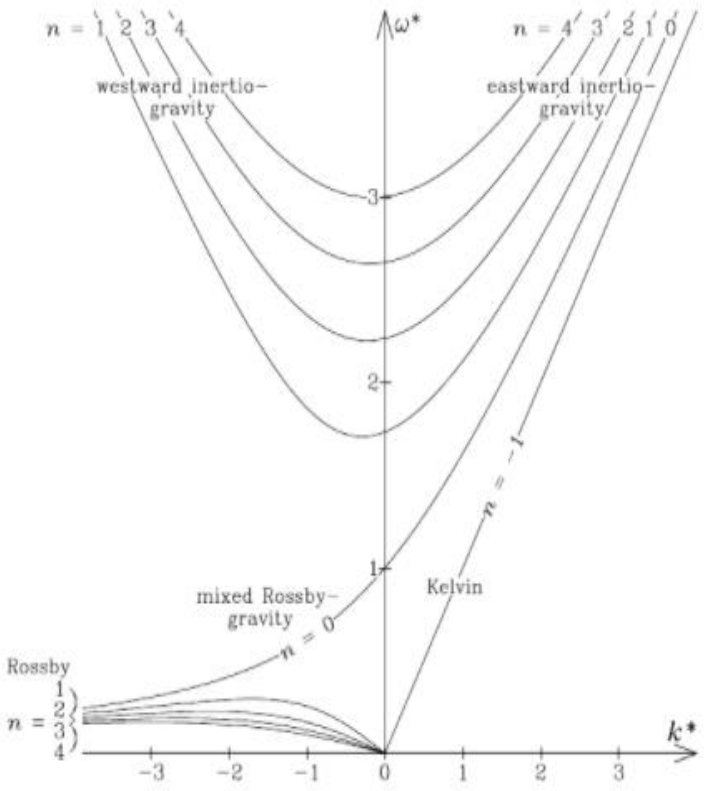

Figure 1: Dispersion curves of all the equatorial wave types. The figure displays the nondimensional eigenfrequencies as a function of the nondiensional zonal wave number. The dimensionless quantities are defined according to (2.3.9). From Kiladis et al. (2009)

Each ω is an eigenvalue of the differential equation (2.3.7) for the meridional structure of the meridional wind. The eigenfunctions of the equation (2.3.7) is the widely known parabolic cylinder functions given by $V_m(y) = H_m(y)e^{(-\frac{y^2}{2})}$; where $H_m(y)$ are the Hermite polynomials of m^{th} degree, which the first three are given by: $H_0(y) = 1;\ H_1(y) = 2y;\ H_2(y) = 4y^2 - 2$. These polynomials satisfy the following recurrence relation $H_{m+1}(y) = 2yH_m - 2nH_{m-1}$. Furthermore, the parabolic cylinder functions form an orthogonal basis on the $L^2(-\infty,\infty)$ vector space.

These wave modes form an orthogonal and complete set in the space of the solutions of the SW system (2.3.4) (Silva Dias and Shubert, 1983). Therefore, the horizontal structure and the time dependence of the first baroclinic and barotropic modes can be written as:

$$\begin{pmatrix} u_1(x,y,t) \\ v_1(x,y,t) \\ p_1(x,y,t) \end{pmatrix} = \sum_{n,k,a} C \begin{pmatrix} -\frac{1}{2}(\omega + k)H_{n+1}(y) - n(\omega - k)H_{n-1}(y) \\ i(\omega^2 - k^2)H_n(y) \\ -\frac{1}{2}(\omega + k)H_{n+1}(y) + n(\omega - k)H_{n-1}(y) \end{pmatrix} e^{-\frac{y^2}{2}} e^{i(kx-\omega t)} \qquad (2.3.11\text{ a})$$

$$\Psi(x,y,t) = Be^{i(kx-\omega_B t)} \sin(ly) \qquad (2.3.11\text{ b})$$

The barotropic wind can be recovered from (2.3.11 b) by the relations:

$$(u,v) = (-\Psi_y, \Psi_x), (u,v) = (-Be^{i(kx-\omega_B t)} \cos(ly), ikBe^{i(kx-\omega_B t)} \sin(ly)) . \qquad (2.3.12)$$

Equations (2.3.11a) and (2.3.11b) are the solutions for the baroclinic and barotropic fields, respectively. The sum is taken over all triples (n,k,a) where n s the meridional wavenumber, k is the zonal wavenumber and a is the wave type (Kelvin, Rossby, eastward and westward inertia-gravity and Yanai) and C is an arbitrary constant that represents the amplitude of the (n,k,a) mode.

Surprisingly, the longitude-time power spectrum of raw atmospheric data, when aproprietely filtered and divided by a background spectrum (see Wheeler and Kiladis 1999 for details), significantly matches the dispersion curves shown in Fig. 1 (see Kiladis et al.2009 and references therein) despite the fact these dispersion curves are solutions of the SW system for a dry dynamics linearized around a motionless state. The only feature appearing in the raw data power spectrum that is not a solution of (2.3.6) is associated with the MJO activity.

2.3.1 Nonlinearity and diabatic forcing

Equation (2.3.11) represents the solutions of (2.3.6) and (2.3.1), which constitute the linearized and unforced version of system (2.2.3). In the linear theory, the superposition principle is valid, that is, given two eigensolutions of a wave equation their linear combination is also a solution. Each eigenmode labeled by the triplet (n,k,a) is a separate solution of the linearized system. However, in the full equations (2.2.3) there are two mechanisms that can break down the independence of the eigenmodes: the nonlinearity and the moist convection. Before obtaining our reduced toy model that considers these two mechanisms, for clarity of exposi-

tion we first illustrate their roles in coupling different eigenmodes separately. As will be shown below, the nonlinearity can couple two equatorial wave modes with a barotropic Rossby wave mode in interacting triads, whilst the moist convection may couple different equatorial wavemodes in duets. In addition, the moist deep convection forcing may also play an important role in the nonlinear triad interactions by modifying the linear eigenfrequencies of the equatorial wave modes.

2.3.2 Nonlinearity

Let us consider the dimensionless form of the nonforced version of the nonlinear evolution equations for the baroclinic and the barotropic modes:

$$\frac{\partial V_1}{\partial t} + yV + \nabla p_1 = -V \bullet \nabla V_1 - V_1 \bullet \nabla V$$
$$\frac{\partial p_1}{\partial t} + div V_1 = -V \bullet \nabla p_1 \qquad \text{(2.4.1 a,b,c)}$$
$$\frac{\partial \Delta\Psi}{\partial t} + \frac{\partial \Psi}{\partial x} = -\left[V_1 \bullet \nabla curl V_1 + 2 curl V_1 div V_1 - V_1^{\perp} \bullet \nabla div V_1\right] - J(\Psi, \Delta\Psi)$$

where we have written the equation for the barotropic mode in terms of the vorticity conservation, with J corresponding to the Jacobian operator. The nondimensionalization of the equations above has been done by considering the equatorial Rossby deformation radius $L = (\frac{c}{\beta})^{\frac{1}{2}}$ as the length-scale and the inverse of the Coriolis parameter, $T = (c\beta)^{-\frac{1}{2}}$, as time-scale, as well as c and c^2 for velocity and pressure scales, respectively. The nonlinearities appearing on the right hand side of (2.4.1) are quadratic. Quadratic nonlinearity is a common feature of fluid dynamics equations due to the advection term of the material derivative. In equation (2.4.1a), the nonlinear terms represent the advection of the baroclinic wind by the barotropic wind and vice-versa, while in equation (2.4.1b) is the advection of the pressure field by the barotropic wind. In contrast, only the self-interactions involving the barotropic and baroclinic components of the wind field contribute to the time evolution of the barotropic mode. One of the main hyphotesis of the present work is referred to the well-kown weakly nonlinear regime, i.e., the regime in which the eigenmodes of the linear system dominate the

dynamics on a time-scale of the order of a complete oscillation of the wave, and the nonlinearity is felt by the system only in a much longer timescale than the characteristic oscillation periods of the waves involved. In addition, the (x, y) structure of the waves is preserved in this regime, and the nonlinearity acts only to make the wave amplitudes to change in time due to the energy exchanges among different modes. Recall that $V_1 = (u_1, v_1)$ and $V = (u, v)$ refer to the baroclinic and barotropic horizontal wind fields, respectively.

From the infinite set of possible eigensolutions given by (2.3.11), as discussed in Chapter 1, our toy model of the MJO activity will consider only an interacting triad composed of an equatorial Rossby mode, an equatorial Kelvin wavemode and a barotropic Rossby mode, since a single interacting triad constitutes the elementary form of nonlinearity manifestation and, in addition, these wave modes are known to play important roles in different features of the MJO. In later sections we will also include an equatorial inertia-gravity mode, which will be coupled with the equatorial Rossby mode through the diurnal cycle of the diabatic forcing. Thus, to illustrate how the nonlinearity works in our barotropic-first baroclinic truncated Boussinesq model, let us consider the following ansatz:

$$\Psi(x,y,t) = B(t)e^{i(k_B x - \omega_B t)} \sin(l_B y) \qquad \text{(2.4.2 a,b)}$$

$$\begin{pmatrix} u_1(x,y,t) \\ v_1(x,y,t) \\ p_1(x,y,t) \end{pmatrix} = K(t)\begin{pmatrix} \hat{u}_K \\ \hat{v}_K \\ \hat{p}_K \end{pmatrix}(y)e^{i(k_K x - \omega_K t)} + R(t)\begin{pmatrix} \hat{u}_R \\ \hat{v}_R \\ \hat{p}_R \end{pmatrix}(y)e^{i(k_R x - \omega_R t)}$$

In the equations above, the subscript K, R and B refer to the equatorial Kelvin, Rossby and barotropic Rossby modes, respectively, with K(t), R(t) and B(t) representing their respective time-evolving amplitudes. Substituting the ansatz (2.4.2) into equations (2.4.1), making use of the linear eigenvalue problem (2.3.6) and the barotropic Rossby mode dispersion relation (2.3.3), the orthogonality of the trigonometric functions on the $[0,2\pi]$interval and the orthogonality of the equatorial mode eigenfunctions, we obtain a set of three ODEs for the time evolution of the wave amplitudes:

$$E_K \frac{dK}{dt} = \sigma_K^{RB} B R^* e^{i\Delta\omega t};$$
$$E_R \frac{dR}{dt} = \sigma_R^{KB} B K^* e^{i\Delta\omega t}; \qquad (2.4.3\ a,b,c)$$
$$(k^2 + l^2)\frac{dB}{dt} = \sigma_B^{KR} R K e^{-i\Delta\omega t}.$$

In the equations above, $\Delta\omega = \omega_B - \omega_K - \omega_R$ is the mismatch among the mode eigenfrequencies of the triad, E_j , j = K or R, refer to the intrinsic energy norm of each equatorial mode, and σ_K^{RB}, σ_B^{RK} and σ_R^{KB} are the nonlinear coupling coefficients, which measure the projection of the nonlinear terms involving products of two modes onto a third mode, given by:

$$\sigma_K^{RB} = -\int_{-\infty}^{\infty}[u_B ik_R u_R + v_B \frac{du_R}{dy} + CP]u_K(y)dy - \int_{-\infty}^{\infty}[u_B ik_R v_R + v_B \frac{dv_R}{dy} + CP]v_K^*(y)dy -$$
$$\int_{-\infty}^{\infty}[u_B ik_R p_R + v_B \frac{dp_R}{dy}]p_K(y)dy. \qquad (2.4.4a)$$

where * indicate complex conjugation and CP means cyclic permutation. The coefficient σ_K^{RB} can be simplified recalling that $v_K = 0$, while the coefficient σ_R^{KB} can be obtained by just relabling $R \to K, K \to R$. On the other hand, the coupling coefficient σ_B^{RK} is given by:

$$\sigma_B^{RK} = \int_{-\infty}^{\infty}\{\sin(l_B y)\left\{u_R ik_K \varsigma_K + v_R \frac{d\varsigma_K}{dy} + 2\varsigma_R[ik_K u_K + \frac{dv_K}{dy}]\right\}$$
$$-V_R^{\perp} \bullet [-k_K^2 u_K + ik_K \frac{dv_K}{dy}, ik_K \frac{du_K}{dy} + \frac{d^2 v_K}{dy}]^T + CP\}dy \qquad (2.4.4b)$$

where $\varsigma_j = ik_j v_j - \frac{du_j}{dy}$.

To obtain equation (2.4.4), the following interaction condition was used:

$$\int_0^{2\pi} e^{i(k_R + k_K - k_B)x} dx = \begin{cases} 0 & k_R + k_K - k_B \neq 0 \\ 2\pi & otherwise. \end{cases} \qquad (2.4.5)$$

The relation above is called resonance condition in space, which is automatically satisfied in this work by the choice of the interacting modes.

As mentioned earlier, in the weakly nonlinear regime the wave amplitudes evolve in a longer time-scale than the corresponding wave phases. Consequently, when $\Delta\omega$ is large, the highly oscillatory factor on the RHS of (2.4.3) inhibits the energy exchanges among the waves. In this sense, the smaller the mismatch among the eigenfrequencies of the triad components, the stronger the amplitude (energy) modulations. The maximum amplitude (energy) variation occurs when the triad is resonant ($\Delta\omega = 0$). As will be shown in Chapter 3, for planetary-scale waves, the dry dynamics governed by system (2.4.3) exhibits very small energy modulations because the mismatch frequency associated with interacting triads of planetary-scale equatorial Rossby, Kelvin and barotropic Rossby waves is large in general. However, as will be demonstrated in the next section, the stationary harmonic of the diurnal cycle of diabatic heating reduces the time-frequency of the equatorial wave modes, specially the Kelvin mode. Consequently, depending on the moisture content, the latent heat forcing may lead such triads to match the resonance condition and, thus, undergo significant nonlinear energy exchanges.

The total energy of the triad equations (2.4.3a, b, c) is conserved if the coupling coefficients satisfy the relation:

$$\sigma_K^{RB} + \sigma_R^{KB} - \sigma_B^{KR} = 0 .$$

2.3.3 Diabatic Forcing:

Latent heat release from condensation of water vapor, into liquid water is the major source of energy in the tropical belt. Additionally, the presence of water vapor strongly influences the large-scale wave dynamics. Dias and Paulius (2009) showed the decrease of the phase velocity of an equatorial wave when it gets inside a moist region like the ITCZ. Two main features of tropical dynamics with effects on weather and climate around the globe exist because of the interaction between moist convection and wave dynamics, the CCEW (convectively coupled equatorial waves) (Wheeler and Kiladis, 1999; Kiladis et al., 2009) and the MJO itself in which moist convection plays a key role in any of its theoretical models (Wang, 2005; Wang and Chen, 2016).

A simple setup is adopted here to analyze the interaction of dry wave dynamics with moist convection. In this context, two effects will be shown, the change in the eigenfrequency of the linear waves associated with the amount of water vapor and the linear duet coupling of equatorial waves due to the meridional gradient of water vapor concentration where the magnitude of the coupling depends on the the amount of vapor as well.

The mechanism of changing the wave phase velocity has an additional effect that is important for the nonlinear wave dynamics. Indeed, as discussed in the previous section, in the weakly nonlinear regime, the nonlinear triad interaction is more effective when the waves are close to resonance. On the other hand, one can observe that for a fixed k (wavenumber), if the phase velocity changes the frequency of the waves changes as well, since $c = \frac{\omega(k)}{k}$. Consequently, in the moist dynamics the reduction of the wave speed may allow for nonlinear resonances that are absent in the dry dynamics i.e, water vapor can change the frequency of the waves such that it may allow a wave triad to match the resonance condition.

To illustrate the role of moist convection in the dynamics of the equatorial wave modes in a simplified fashion, let us consider the diabatic version of the linearized equations (2.3.4 a,b,c) for the first baroclinic mode evolution. In dimensionless form, these equations are written as:

$$\frac{\partial \mathrm{V}_1}{\partial \mathrm{t}} + \mathrm{y}\mathrm{V}_1^{\perp} + \nabla \mathrm{p}_1 = 0\,;$$
$$\frac{\partial \mathrm{p}_1}{\partial \mathrm{t}} + \mathrm{div}\mathrm{V}_1 = -\mathrm{S}_\mathrm{q}\,. \qquad \text{(2.4.6 a,b)}$$

Recall that S_q in the equation above (2.4.6b) is proportional to the projection of the vertical derivative of diabatic heat source onto the first baroclinic mode eigenfunction:

$$S_q = \frac{gL_V H\dot{Q}_Z(x,y,t)}{\pi C_p \theta_0} \qquad (2.4.7)$$

where $\dot{Q}_Z(x,y,t)$ is the projection of the vertical gradient of the heat releasing rate onto the first baroclinic mode. Additionally, the wave-CISK theory assumes that $\dot{Q}_Z(x,y,t)$ is proportional to the convergence of horizontal wind in the lower troposphere. Mathematically:

$$\dot{Q}_Z(x,y,t) = -Q_0 f(t) q(y) \int_0^{z_{NCL}} div V_H dz \qquad (2.4.8)$$

in which the minus sign implies convergence of the horizontal wind and ZNCL $\approx 2km$ is the height of cloud base. Q_0 is the maximum value of the background specific humidity, which depends on the global average temperature by the Clausius-Clayperon equation, while q(y) and f(t) represent its spatial and time variabilities, respectively. It is a major assumption of this work that increasing the temperature of the troposphere and oceans results in more water vapor in the atmosphere. The rise in the amount of water vapor increases precipitation, which in turn increases latent heat release. To mimic the climatological spatial distribution of moisture in the atmosphere, with its maximum along the intertropical convergence zone (ITCZ), the meridional structure of the forcing is defined as a gaussian centered at equator. In dimensionless units, it can be expressed as:

$$q(y) = e^{-\frac{y^2}{2}} \qquad (2.4.9)$$

which in dimensional units refers to have the variance given by the equatorial Rossby radius $(c\beta)^{-\frac{1}{2}} \approx 1500km$. Raupp and Silva Dias (2010) have explored the effect of changing the position of the ITCZ function defined above on the wave interactions. They showed that as the position changes the strenght of the linear and the nonlinear coupling coefficients changes as well, which implies a sensitivity of the wave interactions to the meridional position of the heat forcing. Nevertheless, as the goal of this work is to analyse the effect of changing the moisture content on the wave interactions, we strict to the case where the ITCZ function is centered at the equator. In addition, by assumption the forcing has no zonal structure. The temporal dependence is defined to represent the diurnal cycle of the convective heating. In this way, we have set f(t) by two functions that mimic different aspects of diurnal cycle of convection: i) a full wave rectified sine and ii) a half wave rectified sine:

$$f(t) = \left|\sin(\Omega t)\right| \qquad (2.4.10\ a)$$

$$f(t)=\begin{cases}\sin \Omega t & 0 \le t < \dfrac{\tau}{2} \\ 0 & \dfrac{\tau}{2} < t < \tau\end{cases} \qquad (2.4.10\ b)$$

where $\Omega = \dfrac{2\pi}{\tau}$ indiates the frequency of the diurnal cycle and τ = the duration of the day in dimensionless units, that is $\approx \dfrac{24h}{T_E} \approx 2.9$. By assumption we choose to set the diurnal cycle with wavenumber equals zero as if we were looking the whole time to the place where convection occurs. However, the k=1 zonal structure would be more realistic to mimic the diurnal cycle resulting from solar forcing and will be analysed in a future work.

Let us now Fourier expand these two functions used here for the time dependent part of the heat forcing:

$$\left|\sin(\Omega t)\right| = \frac{2}{\pi} - \frac{4}{3\pi}\cos(\frac{2\pi}{\tau}t) + ... \qquad (2.4.11a)$$

$$\begin{cases}\sin \Omega t & 0 \le t < \dfrac{\tau}{2} \\ 0 & \dfrac{\tau}{2} < t < \tau\end{cases} = \frac{1}{\pi} + 0.5\sin(\frac{2\pi}{\tau}t) + ... \qquad (2.4.11b)$$

In the expansions above, only the first two terms are considered here, which will be labeled hereafter as the stationary and first or transient harmonics, respectively. Combining the elements of the Fourier expansion of the full rectified sine function, the heat forcing can be expressed as:

$$\dot{Q}_Z(x,y,t) = -Q_0 \sin(\frac{\pi z_{NCL}}{H})[\frac{2}{\pi} - \frac{4}{3\pi}\cos(\frac{2\pi}{\tau}t)]e^{-\frac{y^2}{2}} div V_1 \qquad (2.4.12)$$

where we have used Galerkin expansion (2.2.2 a) of the horizontal wind as well as the divergenceless condition of the barotropic mode.

Using (2.4.12), one can rewrite S_q as:

$$S_q = \frac{-gL_V Q_0 H[\frac{2}{\pi} - \frac{4}{3\pi}\cos(t)]e^{-\frac{y^2}{2}} \sin(\frac{\pi z_{NCL}}{H}) div V_1}{C_p \theta_0 \pi} \quad (2.4.13)$$

Therefore, equation (2.4.6b) in dimensionless units becomes:

$$\frac{\partial p_1}{\partial t} + div V_1 = \frac{gL_V Q_0 H[\frac{2}{\pi} - \frac{4}{3\pi}\cos(\frac{2\pi}{\tau}t)]e^{-\frac{y^2}{2}} \sin(\frac{\pi z_{NCL}}{H}) div V_1}{c^2 C_p \theta_0 \pi} \quad (2.4.14)$$

Note that: $\frac{gL_V Q_0 H \sin(\frac{\pi z_{NCL}}{H})}{C_p \theta_0 \pi}$ has dimension of velocity squared. Consequently, labling

$$c_m^2 = \frac{gL_V Q_0 H \sin(\frac{\pi z_{NCL}}{H})}{C_p \theta_0 \pi} \quad (2.4.15)$$

and considering only the stationary mode, it follows that the correction of the characteristic linear wave speed of the equatorial wave modes can be expressed as a phase velocity modified by the moist convection effect (assuming for instance no meridional and time dependencies of the term multiplying the horizontal divergence on equation 2.4.14 to simplify the illustration):

$$c_* = (1 - \frac{2c_m^2}{\pi c^2}) \quad (2.4.16)$$

From (2.4.16), it is possible to visualize a basic mechanism by which global warming can influence the wave dynamics. The value of c_m^2 depends explicitly on Q_0, which, in turn, is a exponential function of temperature according to Clausius-Clayperon equation. One obvious aspect is that this correction more significantly affects modes characterized by a high divergence, such as Kelvin and inertio-gravity waves. The reintroduction of the meridional structure and time dependence allows for coupling between different equatorial modes and, as consequence, rotational modes such as equatorial Rossby waves can also be affected.

Let us now consider again the meridional and time dependencies of the parametric heat forcing to illustrate the effect of the moist convection heating on the equatorial wave dynamics in a more complete picture. For this purpose, it is convenient to express the first (transient) harmonic of the diurnal cycle of the heating in the exponential forms:

$$\cos(\frac{2\pi}{\tau}t)=\frac{e^{i\frac{2\pi}{\tau}t}+e^{-i\frac{2\pi}{\tau}t}}{2} \quad \text{and} \quad \sin(\frac{2\pi}{\tau}t)=\frac{e^{i\frac{2\pi}{\tau}t}-e^{-i\frac{2\pi}{\tau}t}}{2i}.$$

The following development will be explicit only for the first harmonic of fully rectified wave, following the approach of Raupp and Silva Dias (2010). The existence of such oscillation in time renders possible to satisfy resonance condition in a non trivial fashion, allowing for the coupling of two distinct modes. In fact, as the equatorial inertia-gravity waves exhibit periods close to the diurnal cycle, the mismatch between the frequencies of the equatorial gravity mode and the diurnal cycle is compatible with the frequency range of equatorial Rossby modes, making possible the existence of resonant interaction between equatorial Rossby and gravity waves through the transient harmonic of the diurnal forcing (Raupp and Silva Dias 2010). This setup is of interest here because it provides a mechanism through which high frequency motions embedded in the MJO can influence the behavior of the large-scale envelope of the MJO. Several studies have shown the importance of understanding the transport of energy and momentum from mesoscale high frequency convective flow to large-scale slow motion of the MJO (see, for instance, Stechmann and Majda 2011; Majda 2007).With these considerations, let us consider the following ansatz:

$$\begin{pmatrix} u_1(x,y,t) \\ v_1(x,y,t) \\ p_1(x,y,t) \end{pmatrix} = R(t)\begin{pmatrix} \hat{u}_R \\ \hat{v}_R \\ \hat{p}_R \end{pmatrix}(y)e^{i(kx-\omega_R t)} + G(t)\begin{pmatrix} \hat{u}_G \\ \hat{v}_G \\ \hat{p}_G \end{pmatrix}(y)e^{i(kx-\omega_G t)} + c.c \ .$$

Substituting the ansatz above into equations (2.4.14) and (2.4.6a), making use the fact that the meridional structure functions satisfy the eigenvalue problem (2.3.6), as well as the orthogonality of these eigenfunctions, we obtain:

$$\begin{aligned} E_G\frac{dG}{dt} - i\omega_G G(t)\eta_{GG} &= i\omega_R R(t)\eta_{RG} \\ E_R\frac{dR}{dt} - i\omega_R R(t)\eta_{RR} &= i\omega_G G(t)\eta_{GR} \end{aligned} \qquad \text{(2.4.17 a,b)}$$

where:

$$\eta_{RG}=\frac{2gL_V Q_0 H\sin(\frac{\pi z_{NCL}}{H})}{3\pi C_P\theta_0\pi}\int_{-\infty}^{\infty} e^{-\frac{y^2}{2}}\hat{p}_R(y)\hat{p}_G^*(y)dy;$$

$$\eta_{GR}=\frac{2gL_V Q_0 H\sin(\frac{\pi z_{NCL}}{H})}{3\pi C_P\theta_0\pi}\int_{-\infty}^{\infty} e^{-\frac{y^2}{2}}\hat{p}_G(y)\hat{p}_R^*(y)dy;$$

$$\eta_{RR}\frac{gL_V Q_0 H[\frac{2}{\pi}]\sin(\frac{\pi z_{NCL}}{H})}{C_P\theta_0\pi}\int_{-\infty}^{\infty}e^{-\frac{y^2}{2}}\hat{p}_R(y)\hat{p}_R^*(y)dy\,;$$

where η_{GG} can be obtained by relabling R $\rightarrow$G and, as the pressure fields are real, it follows that $\eta_{RG}=\eta_{GR}$.

In the equations above, one can see that the role of the stationary harmonic is to alter the natural frequency of oscillation of each of the wave modes. This is a somewhat remarkable result. It shows that the presence of meridional gradient of moisture changes the phase velocity of the waves. To make more clear the role of the stationary harmonic of the temporal moisture function in modifying the eigenfrequencies of the equatorial modes, we make the following transformation of variables $R(t)\rightarrow R(t)e^{i\omega_R t}$, $G(t)\rightarrow G(t)e^{i\omega_G t}$. In this way, equations (2.4.17a, b) now read:

$$\begin{aligned}&E_G\frac{dG}{dt}+i\omega_G(1-G(t)\eta_{GG})=i\omega_R R(t)\eta_{RG}\,;\\&E_R\frac{dR}{dt}+i\omega_R(1-R(t)\eta_{RR})=i\omega_G G(t)\eta_{GR}\,.\end{aligned}\qquad(2.4.18\ a,b)$$

On the other hand, the role of the first (transient) harmonic of the diurnal cycle is to promote a linear coupling between the Rossby and gravity modes. In the equations above, we have assumed the following resonance condition is satisfied:

$$\omega_G\pm\omega_R\pm\frac{2\pi}{\tau}=0\qquad(2.4.19\ )$$

2.4 Combining the effects of nonlinearity and diabatic forcing

Now that we have illustrated the role of the nonlinearity and the diabatic forcing in the wavemodes of system (2.2.3), let us now combine their effects to build our toy model of the MJO activity. This toy model is the object of analysis in order to shed some light on the mechanism linking the increase in the average temperature field with other climate changes including extreme events. This toy model will serve as a proxy for the MJO behaviour containing its principal elements: the convectively coupled equatorial Rossby and Kelvin modes as constituting the planetary-scale MJO envelope, the barotropic Rossby mode as the link

between tropics and extratropics and the interaction between large-scale equatorial Rossby and high frequency gravity waves through diurnal cycle simulating the interaction between moist convection and large scale structure of MJO. In this context, to obtain this toy model, we consider the following ansatz:

$$\begin{pmatrix} u_1(x,y,t) \\ v_1(x,y,t) \\ p_1(x,y,t) \end{pmatrix} = R(t)\begin{pmatrix} \hat{u}_R \\ \hat{v}_R \\ \hat{p}_R \end{pmatrix}(y)e^{i(kx-\omega_R t)} + G(t)\begin{pmatrix} \hat{u}_G \\ \hat{v}_G \\ \hat{p}_G \end{pmatrix}(y)e^{i(kx-\omega_G t)} + K(t)\begin{pmatrix} \hat{u}_K \\ \hat{v}_K \\ \hat{p}_K \end{pmatrix}(y)e^{i(kx-\omega_K t)} + c.c \quad (2.5.1a)$$

$$\Psi(x,y,t) = B(t)e^{i(k_B x-\omega_B t)}\sin(l_B y) \quad (2.5.1\ b)$$

Thus, inserting (2.5.1) into (2.2.3) yields:

$$\begin{aligned} &E_K\frac{dK}{dt} - i\omega_K(1-K(t)\eta_{kk}) = \sigma_K^{RB}BR^*; \\ &E_R\frac{dR}{dt} - i\omega_R(1-R(t)\eta_{RR}) = \sigma_R^{KB}BK^* + i\omega_G G(t)\eta_{RG}; \\ &(k_B{}^2 + l_B{}^2)\frac{dB}{dt} = \sigma_B^{KR}RK\ ; \\ &E_G\frac{dG}{dt} - i\omega_G(1-G(t)\eta_{GG}) = i\omega_R R(t)\eta_{GR}. \end{aligned} \quad (2.5.2a,b,c,d)$$

Chapter 3: RESULTS

As demonstrated in the previous chapter, one of the effects of the parametric thermal forcing considered here is to reduce the eigenfrequency of the equatorial wave-modes. This effect is assonated with the stationary harmonic of the time dependent part of the moisture function and is evidenced by equations (2.4.18a, b). In fact, the equivalent of (2.4.17) for the Kelvin wave is given by:

$$\frac{dK}{dt} = i\omega_K K \frac{gL_V Q_0 H[\frac{2}{\pi}]\sin(\frac{\pi z_{NCL}}{H})}{C_P \theta_0 \pi} \int_{-\infty}^{\infty} e^{-\frac{y^2}{2}} \hat{p}_K(y)\hat{p}_K^*(y)dy \qquad (3.1)$$

In this way, with the transformation of variable for the Kelvin mode spectral coefficient, $K(t) \to K(t)e^{i\omega_K t}$, it is possible to show that the effective time-frequency of the Kelvin mode canbe modified from its eigenvalue due to moisture, vis.,

$$\omega_K = \omega_K (1 - \frac{gL_V Q_0 H[\frac{2}{\pi}]\sin(\frac{\pi z_{NCL}}{H})}{C_P \theta_0 \pi} \int_{-\infty}^{\infty} e^{-\frac{y^2}{2}} \hat{p}_K(y)\hat{p}_K^*(y)dy) \qquad (3.2)$$

Equation (3.2) indicates that the amount of water vapor Q_0 determines the intensity of the wave slow down. This effect is illustrated in Fig. 2, which shows the computation of the time-frequency of the equatorial Kelvin mode according to (3.2), as well as its phase speed $c_{pK} = \frac{\omega_K}{k_K}$ for several values of Q_0 . For the parameters N = $0.01s^{-1}$ and H = 18Km, it follows that the dry Kelvin wave speed is $c_{pK} = c \approx 50m/s$. Nevertheless, one notices from Fig. 2 that the propagation speed of the equatorial Kelvin mode is substantially reduced as Q_0 increases, and so are Kelvin mode eigenfrequencies for all the wavenumbers. In fact, Fig. 2 shows that for k (wavenumber) = -0.5, the frequency lessens from 0.5 (dry case) to approximately 0.15. Thus, the magnitude of the decrease of the frequency astonishes. Nevertheless, the results displayed in Fig. 2 are compatible with previous theoretical investigations on con-

vectively coupled equatorial Kelvin waves (see, for instance, Chang and Lim 1988; Wang 1988; Yang and Rui 2000; Silva Dias and Pauluis 2009).

The same effect of the stationary harmonic of moist convection in reducing the mode time-frequency holds for the equatorial Rossby wave as well, but with a lesser intensity (figure not shown). The effect is more pronounced in the divergent modes than in the rotational modes because of the parametrization of the diabatic forcing considered here, which relies on the divergence field of the waves. The effect of this slowdown of the equatorial wave modes due to their coupling with moist convection is to allow the possibility of resonant triads involving equatorial Rossby, equatorial Kelvin and barotropic Rossby modes. To demonstrate this effect, we have adopted a graphical approach to seek resonant triads involving planetary-scale equatorial Rossby and Kelvin modes, either coupled or uncoupled with moist convection, and a barotropic Rossby mode. This graphical approach consists in changing the origin of the dispersion curve of one mode type (equatorial Kelvin). Then, the produced intersection (if occurs) with the dispersion curve (equatorial Rossby) to the wavenumber of interest along the dispersion curve of the barotropic Rossby wave determines the set of three wave-modes satisfying the resonant triad conditions (see, for instance, Raupp et al. 2008; Ramirez et al. 2017). This procedure is illustrated in Fig. 3 for the dry case as well as for the case in which the two equatorial modes are coupled with moisture for different values of the parameter Q_0.

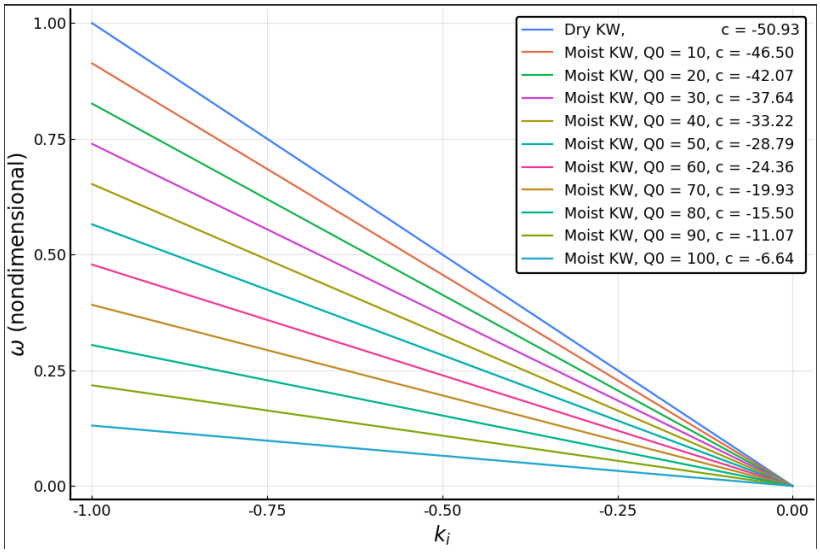

Figure 2: Change in Kelvin wave frequency under increase in atmospheric water vapor, the legend in the right upper corner display the amount of water vapor in g/kg as well the propagation speed of the wave.

Fig. 3 shows that such resonant interaction involving these three wave types no longer exists in the dry case. Indeed, one notices that there is a threshold value of Q_0 that allows resonant triads involving these three wave types, which corresponds to the value of Q_0 for which the dispersion curve of the equatorial Rossby wave touches the maximum point of the barotropic wave dispersion curve. Beyond this threshold, Fig. 3 shows that there are at least two barotropic Rossby wave modes that constitute resonant triads with the equatorial Rossby and Kelvin modes, for the specified wavenumber of the Kelvin wave chosen in Fig. 3. For higher values of the moisture content, the equatorial Rossby wave dispersion curve gets closer to the dispersion curve of the barotropic Rossby wave, which implies that resonances become more possible.

As discussed earlier, in the weakly nonlinear regime, the triad interaction becomes more expressive, with the modes undergoing stronger energy (amplitude) modulations, when the mismatch among the mode frequencies is close to zero, characterizing the so-called resonant triads. Therefore, we expect that for triads composed of a barotropic Rossby mode and equatorial Rossby and Kelvin modes, the moisture content might play an important role in the energy exchanges among these wave modes.

To demonstrate this effect, Fig. 4 shows the result of a numerical integration of the triad system (2.4.3a, b, c) for a representative example composed of a zonal wavenumber 2 Kelvin mode, an equatorial Rossby mode with zonal wavenumber 4 and meridional index n = 1 and a barotropic Rossby mode with zonal wavenumber 2 and meridional wavenumber 2. All the time integrations illustrated in this chapter have been performed with a fourth-order Adams-Bashford scheme with a time step of $10^{-3}s$.

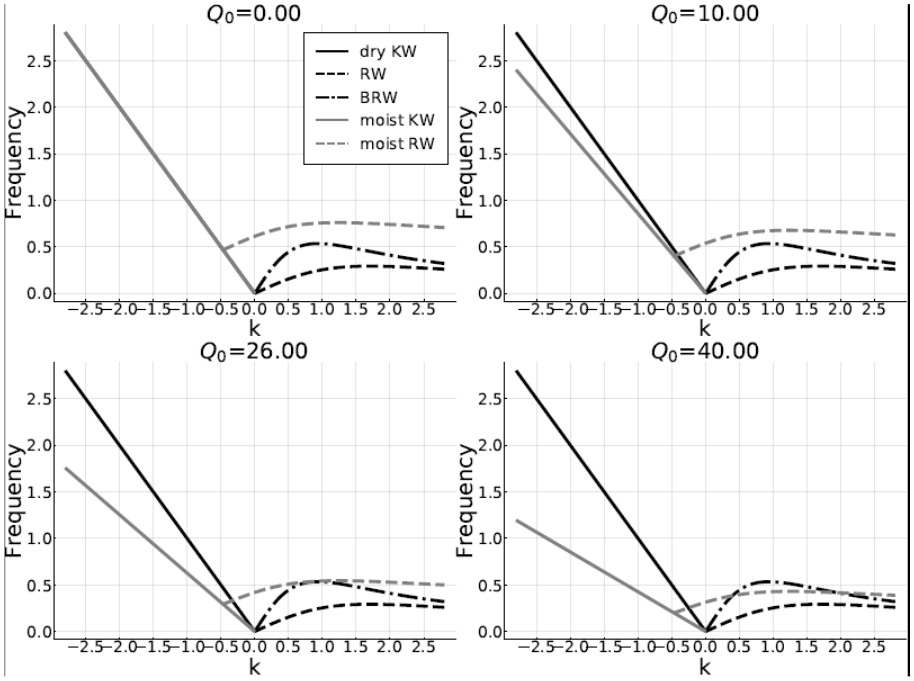

Figure 3: Illustration of the graphical method for searching resonant triads involving equatorial Kelvin,equatorial Rossby and barotropic Rossby waves, for the dry case ($Q_0 = 0$), as well as for the moist dynamics with different values of $\mathbf{Q_0}$. It is shown that the decrease of the frequency of the Kelvin wave renders possible the existence of resonant triads involving these wave types.

The numerical integration displayed in Fig. 4 has been done with the eigenfrequencies of the two equatorial modes being computed through expression (3.2) (both Rossby and Kelvin). This is similar to considering only the stationary harmonic of the Fourier expansion of the time-dependent part of the moisture field, yielding the equatorial gravity mode of system (2.5.2a, b,c, d) to decouple from the waves of the interacting triplet. Thus, Fig. 4 shows the time evolution of the mode energies of the triad for different values of the moisture content parameter Q_0 . It is possible to note that in the dry case ($Q_0 = 0$), the high mismatch among the mode eigenfrequencies for this triad inhibits the energy exchanges among the wave modes. In contrast, in the moist case the energy modulations become more expressive as Q_0 increases. However, for very high values of this parameter (e.g., Q_0 = 79.44 g/Kg illustrated in the last panel), the mismatch gets high again and consequently the magnitude of the energy modulations gets smaller. The value of Q_0 for which this triad is resonant refers to Q_0 =36.47g/Kg (upper right corner). This value of Q_0 is higher than what is frequently observed in the real atmosphere in present climte conditions. However, given the uncertainty level regarding the

climate projections, this value could be representative of the global warming projections related to the least optimistic scenarios of CO2 emissions. Also, the ideia is to show that as the moisture increases the system gets closer to resonance, although it does not necessarily match the condition exactly. Just by approximating from the resonance condition the system exchanges energy more efficiently, which already has an important impact in the atmospheric dynamics. One can observe that this case refers to the strongest energy modulations among the modes.

Another important feature observed in Fig. 4 is that, apart from modifying the magnitude of the energy modulations through the effect on the mismatch of the eigenfrequencies of the triad components, the moisture content also influences the interaction period of the triad (i.e., the period of the energy modulation). In fact, the interaction period relies on the coupling coefficients, which in turn are functions of the eigenfrequencies of the modes of the triad. Thus, as the eigenfrequencies of the equatorial modes are modified by the moisture content, apart from the triad mismatch, the nonlinear coupling constants are affected by changing the moisture content as well.

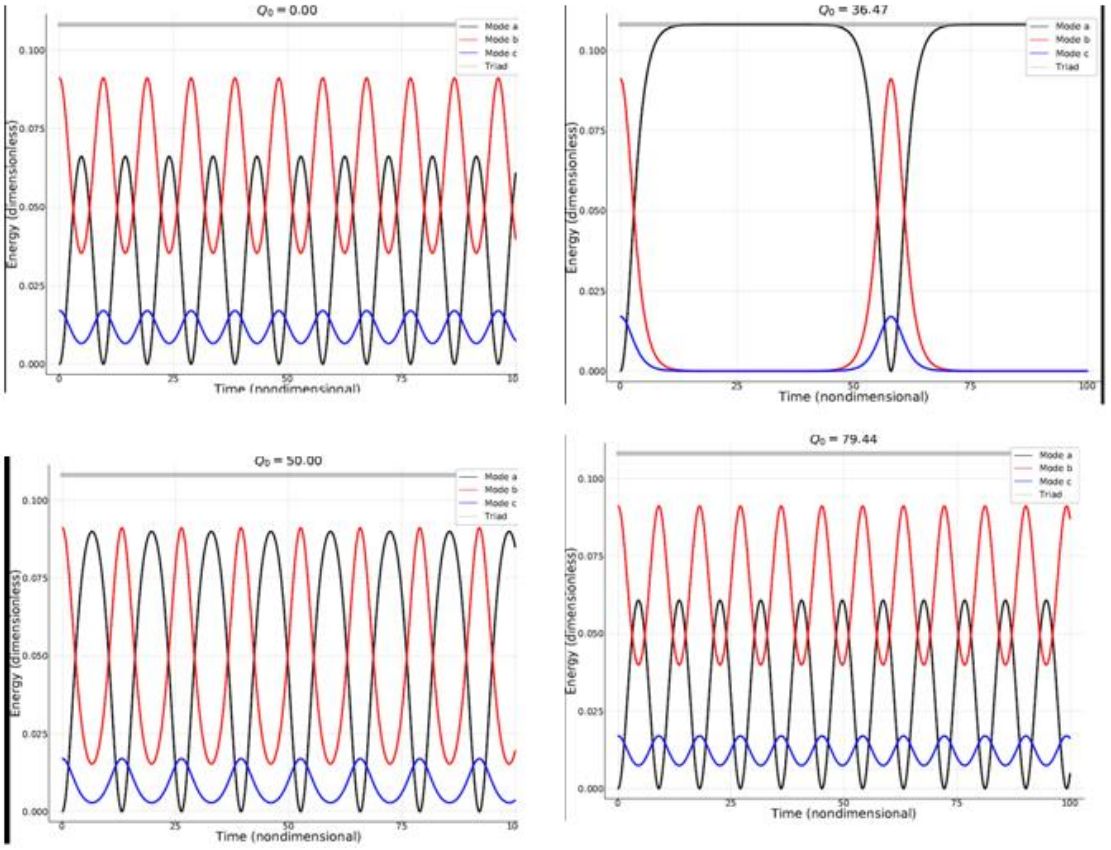

Fig. 4: Time evolution of the mode energies referred to a numerical integration of the triad system(2.4.3a, b, c) for a representative example composed of a zonal wavenumber 2 Kelvin mode, an equatorial Rossby mode with zonal wavenumber 4 and meridional index n = 1 and a barotropic Rossby mode with zonal wavenumber 2 and meridional wavenumber 2. Each panel corresponds to different value of the moisture content: $Q_0 = 0$ (upper left), $Q_0 = 36.47$g/Kg (upper right), $Q_0 = 50$g/Kg (lower left) and $Q_0 = 79.44$g/Kg (lower right).

In order to illustrate the effect of adding the transient harmonic of the diurnal cycle of the convective forcing, Fig. 5 shows the result of the time integration of the reduced system (2.4.17a, b) describing the duet interaction between equatorial Rossby and gravity modes through this transient harmonic of the moisture function. The transient harmonic in this example illustrated in Fig. 5, the equatorial Rossby mode of the triad displayed in Fig. 5 interacts with an eastward propagating inertia-gravity mode with zonal wavenumber 4 and meridional index n = 3. Fig 5 shows the energy exchange between these tow wave modes for different values of the amount of water vapor Q_0. As expected from equations (2.4.17), for $Q_0 = 0$ (dry case) there is no interaction between the two modes, as shown in Fig. 5a (upper left corner). This indicates that what connects these two waves is the presence of water vapor. The presence of moisture is a necessary condition to couple these two modes. In addition, as the

amount of water vapor measured by the parameter Q_0 modifies the time-frequencies of the modes, it determines the possibility of not for these modes to match the resonance condition. This can be verified by comparing the panels b, c and d, where the resonant condition is met in Fig. 5b (upper right corner), for which case the energy modulations are maximal.

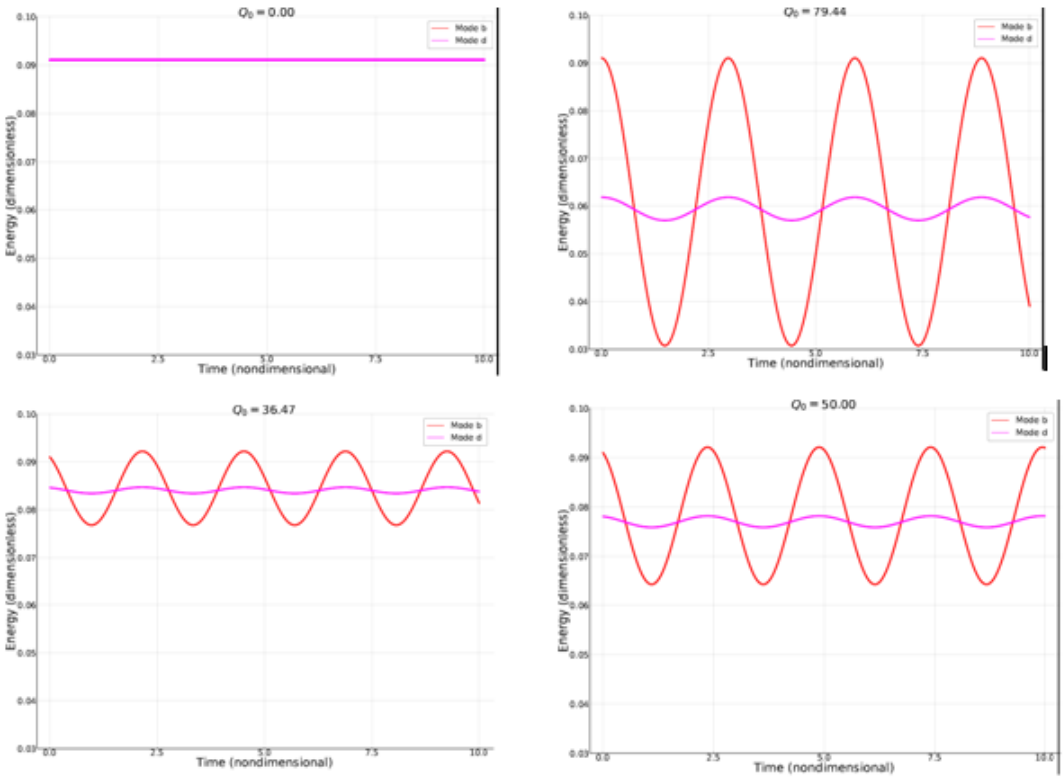

Figure 5: Energy exchange between an Equatorial Rossby (ER) and an equatorial Gravity mode governed by the duet system (2.4.17), for different values of Q_0 . The ER wave is the same interacting triplet mentioned above.

So far we have discussed the effect of moisture on the wave dynamics. It was shown that the moisture reduces the phase speed of the equatorial waves, as illustrated in Fig. 2 for the Kelvin waves. As demonstrated in Fig. 3, this reduction, in turn, allows planetary-scale equatorial Rossby and Kelvin modes to achieve the resonance condition with a barotropic Rossby wave mode in the triad system (2.4.3). Hereafter throughout this chapter we will analyze how the moisture content can affect the dynamics of the triad when a gravity mode is coupled with the equatorial Rossby mode in the four-wave system (2.5.2). Thus, Figures 6-9 show the time integration of the four-wave system (2.5.2a,b,c,d) for the modes composing the

triad interaction illustrated in Fig. 4 coupled with the duet modes displayed in Fig. 5. Thus, the representative example of the four-wave system displayed in these figures is composed of the following eigenmodes:

Mode 1: k1 = -2; n1 = -1 (Kelvin);
Mode 2: k2 = 4; n2 = 1 (Equatorial Rossby)
Mode 3: k3 = k1 + k2; l3 = 2 (barotropic mode);
Mode 4: k4 = -4; n4 = 3 (equatorial gravity);

In the first numerical simulation (Fig. 6) the amplitude of the gravity wave is considered as a free parameter of the four-wave system (2.5.2a,b,c,d) composed of the barotropic Rossby and the equatorial Kelvin, Rossby and gravity modes. One of the effects of increasing the moisture content in the lower troposphere is to enhance the thermodynamic instability of the atmospheric column by creating an upward buoyance force. This is in general measured by the corresponding increase of CAPE (Convective Available Potential Energy). The gravity mode is the wave type that is directly associated with this deep convection process. Moreover, the amplitude of the gravity wave in a region far from equilibrium, such as inside a region of intense deep convection activity, is uncertain. Consequently, it is plausible to explore the dynamics of the four-wave system with a broad range of values for the gravity mode initial amplitude.

Figure 6 shows how the change in gravity wave initial amplitude affects the dynamics of the modes of the triad in the four-wave system (2.5.2a,b,c,d).

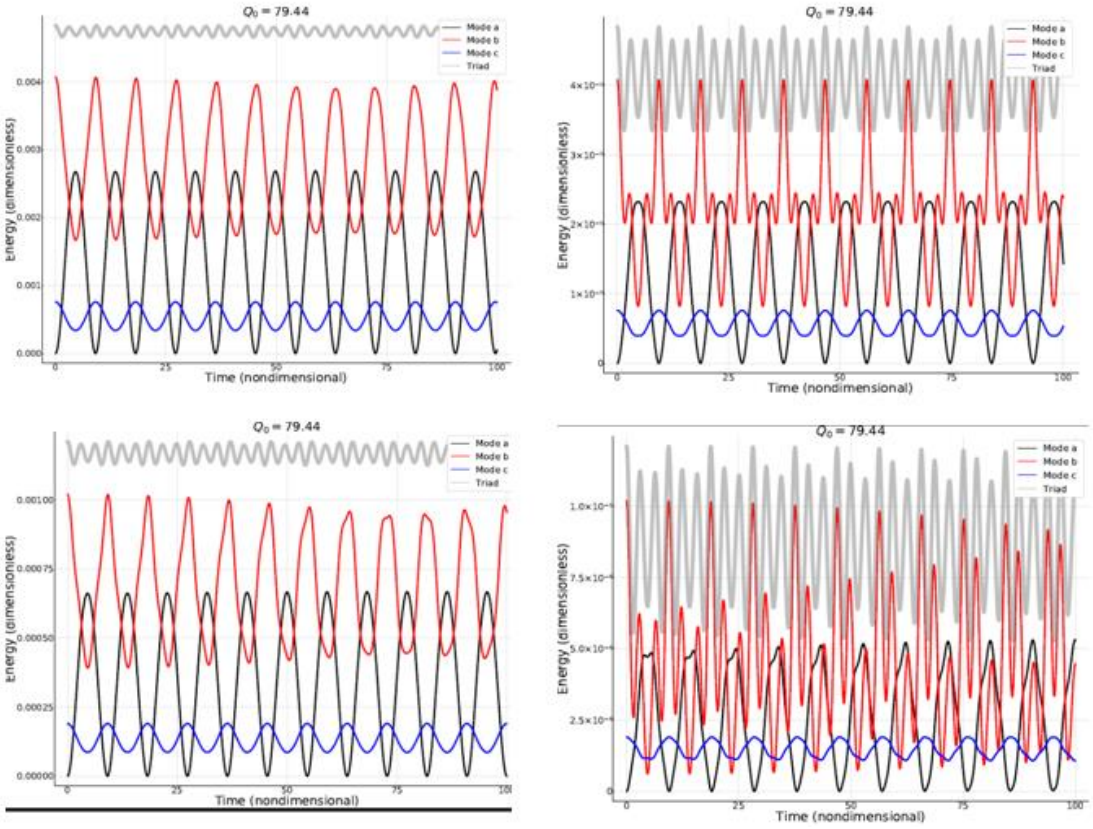

Figure 6: Time evolution of the mode energies of the triad in the four-wave dynamics (2.5.2a,b,c,d). The moisture amount is fixed with the value that leads the duet ER-G to match the resonance condition with the diurnal frequency (Q_0 = 79.44g/Kg), and the corresponding values of the gravity mode initial amplitude are given by: G_0 (upper left), 10 G_0 (lower left), 50G_0 (upper right) and 100G_0 (lower right).

Although the values of 50G_0 and 100G_0 may not be attainable in real atmosphere for present climate conditions, the ideia is to show that as the gravity wave amplitude increases the dynamics of the MJO is altered as well. Considering the uncertainty regarding the possible global warming effect in triggering or enhancing instabilities in the atmosphere, it is not unreasonable to think that gravity wave amplitude might reach very high values in the furute, especially for the least optimistic scenariois of CO2 emissions.

Figure 6 clearly shows that, when the initial gravity wave amplitude is high, which is believed to occur during periods of intense convection activity embedded in the MJO, the gravity mode is able to significantly modulate the energy of the triad. In this case, the energy passes back and forth from the triad to the duet. This has several implications for the dynamics of the atmosphere. In fact, gravity waves are ubiquitous in the atmosphere as they are known to play an important role in the geostrophic adjustment processes, to trigger new con-

vection cells and to transfer momentum to the stratosphere, among other phenomena. Thus, this back and forth energy transfer from the interacting triad to the gravity mode can be regarded as a possible theoretical mechanism for how slow wave modes composing the planetary-scale envelope of the MJO can excite high frequency waves embedded in the MJO and vice-versa.

In the numerical experiment displayed in Fig. 7, the initial amplitude of the gravity mode is fixed in $50G_0$ for clarity of the argument. In this case, the background specific humidity varies from zero (dry case) up to the value of resonance of the duet ER-G with the diurnal cycle (≈79 g/kg).

For $Q_0 = 0$ (dry case), the triplet is decoupled from the gravity mode and what is seen is just the nonlinear triad interaction acting outside the resonance regime. As the parameter Q_0 increases, the triad modes undergo a period-doubling in their energy evolution in time. In Fig. 7b (upper right panel), the interacting triplet is in resonance, which can be seen through the Kelvin (black curve) and Barotropic Rossby (blue curve) wave energies reaching their maximum modulation magnitude. Nevertheless, the total energy of the triplet (gray curve) starts to undergo a little modulation. This modulation of the total triad energy is due to the effect of the gravity wave being coupled with the equatorial Rossby mode. The effect of the coupling with the equatorial gravity mode through the equatorial Rossby mode can also be noticed by the small irregularities in the equatorial Rossby (ER) energy evolution (red curve). In Fig. 7c (lower left panel), the duet ER-Gravity is closer to its resonance condition, which implies that the gravity mode effect on the triplet is more pronounced. This pronounced effect can be noticed through the stronger modulation of total energy of the triad (gray curve) and through the behavior of the ER mode energy. In the last panel (lower right - Fig. 7d), the duet ER-Gravity is in resonance through the diurnal frequency, and the gravity wave energy is most efficiently exchanged with a member of the triplet, what can be clearly seen in the behavior of total triad energy (gray curve). In addition, in the resonance regime of the ER-gravity duet, even the Kelvin mode energy starts to feel the effect of the gravity mode, losing the smoothness of its energy evolution.

Therefore, from the numerical results illustrated in Figure 7, one can see that resonance might be the key feature in the atmospheric wave dynamics, as already noticed from the results presented in Figure 4 for the sole interacting triad. When the value of Q_0 reaches the resonance condition of the triad, the nonlinear triad interaction dominates the 4-wave dynam-

ics. However, as Q_0 increases and is in between the two resonances, it is possible to verify a mixture of effects in which neither the triad nor the duet dominates the 4-wave dynamics. Afterwards, when the parameter Q_0 establishes the duet resonance, the energy modulation of the triad members is significantly affected by the interaction with the duet. Since no triad is isolated in nature, this poses a real challenge for climate research community. In fact, the amount of water vapor in the atmosphere is determinant to know what kind of interaction will dominate the atmospheric dynamics to a second order approximation (since the hypothesis is that in a first order approximation the free linear wave dynamics is supposed to be dominant). This has implications for: (i) the prediction of the energy distribution in the atmosphere, (ii) the MJO teleconnection pattern evolution in the context of a warmer planet, and (iii) the prediction of the MJO itself. Therefore, it is imperative to understand the mechanisms of feedback and maintenance of water vapor in the atmosphere in order to accurately simulate the evolution of the moisture field with global warming. Even in the simplistic model used in the present work, it is possible to grasp the inherently difficulty involved in the climate change projections.

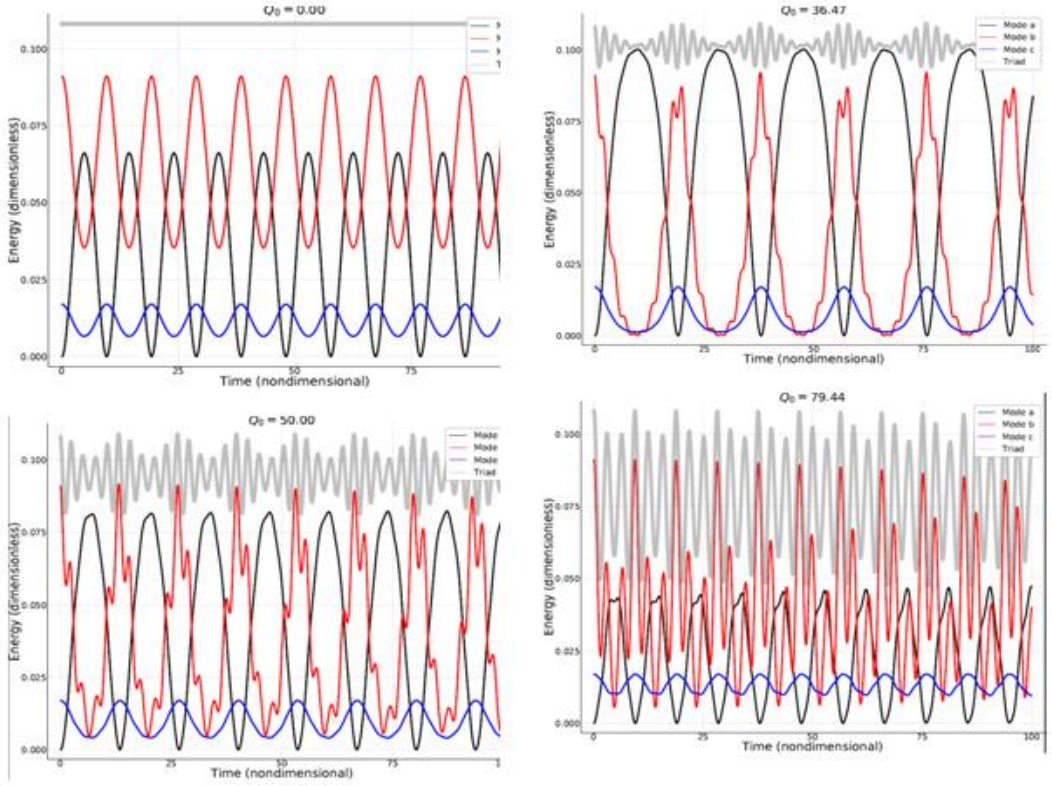

Figure 7: Time evolution of the mode energies of the triad in the four-wave dynamics (2.5.2a,b,c,d), for an initial gravity mode amplitude of $50G_0$ and the following values of Q_0: a) Q_0=0 (upper left), b) Q_0= 36.47 (resonance value for the triad – upper right), c) Q_0=50 (lower left) and d) Q_0= 79.44 (resonance value for the duet ER-G, lower right). The parameter Q_0 is given in g/kg.

Fig. 8 shows the same numerical integration of Fig. 7, but with a reverse perspective. What is shown in Fig. 8 is how the duet ER-gravity is affected by the triplet. In Fig. 8a (upper right panel), as Q_0 = 0, the duet interaction between equatorial Rossby and gravity modes is not affected by the triad interaction, and the duet energy exchange is identical to that predicted by equations (2.4.17). For Q_0 = 36.47g/Kg, Fig. 8b (upper right panel) shows that the triad interaction still dominates the ER mode energy evolution, and the interaction with the gravity mode remains weak, although small perturbations start to appear in the gravity mode energy evolution due to its connection with the ER mode. With the value of Q_0 referred to Fig. 8c (lower left panel), the duet is closer to its resonance condition with the diurnal cycle, and the amplitude of the gravity mode energy modulation becomes more intense, which may yield the loss of smoothness of the ER mode energy evolution.

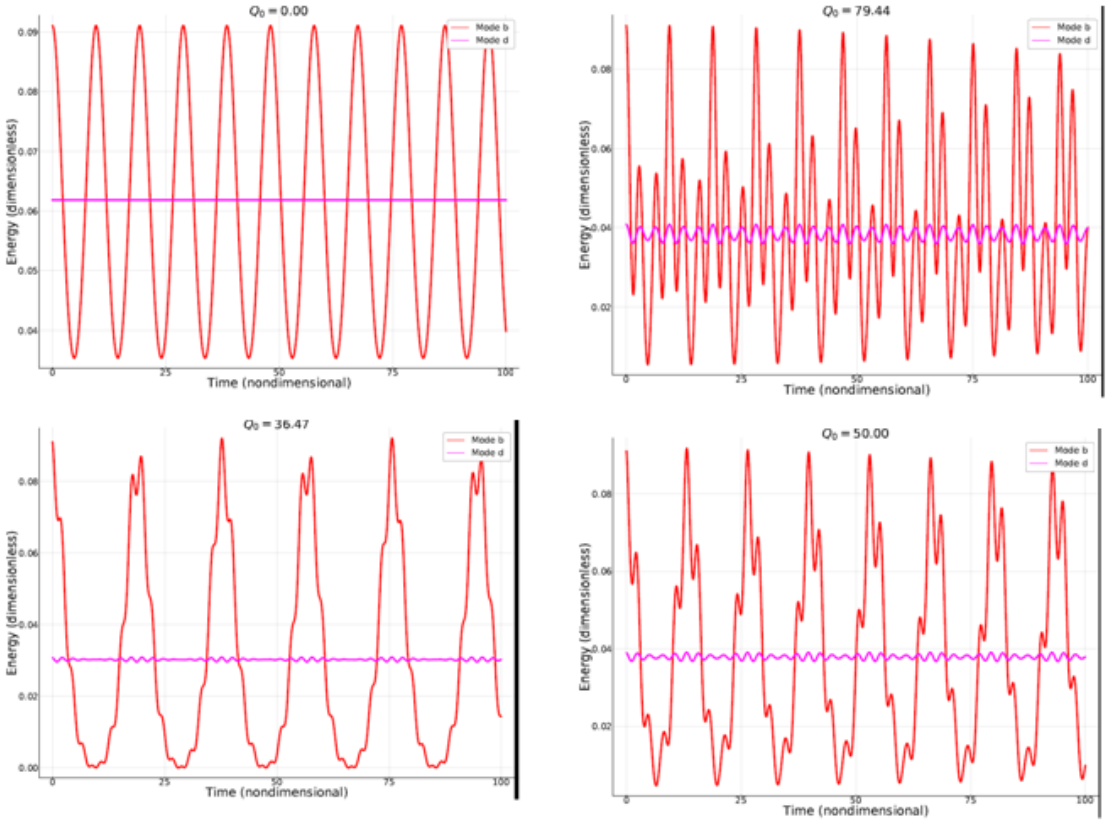

Figure 8: Same numerical integration of Fig. 7, but displaying the energy evolution of the duet modes.

The results displayed in Fig. 8 can also be thought of as a mechanism by which large-scale dynamics can influence high-frequency convection. The ER mode exchanging energy with kelvin and Barotropic Rossby modes can excite a gravity mode and transfer energy from the triad to this wave mode. Comparing Figs. 7 and 8, one can see that the ER mode in the presence of water vapor can transfer energy back and forth from the triad to the gravity mode and vice-versa.

This can be important not only for understanding the MJO dynamics but also for an extremely important process in the distribution of energy in the atmosphere called moist geostrophic adjustment. Any further discussion of this process is outside the scope of this work and will appear in the future suggestions of inquiry.

Fig. 9 shows the phase space perspective of the numerical results presented in Fig.7, illustrating the energy of the equatorial Rossby mode as a function of the Kelvin mode energy.

From this perspective, it is more clear the qualitative change of behavior of the system as the water vapor concentration Q_0 increases. In the absence of water vapor, the system is trapped in a regular oscillation; as water vapor level rises, the oscillation becomes more irregular.

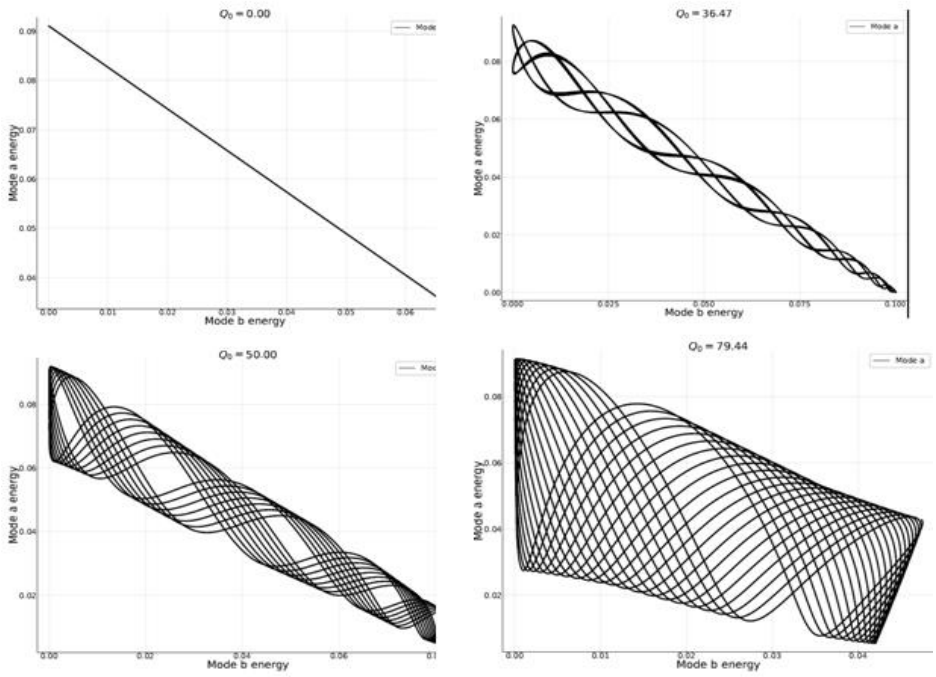

Figure 9: Phase space perspective of the integration displayed in Fig. 7, displaying the energy of Kelvin mode as a function if the ER mode energy.

Fig. 10 illustrates the results of a numerical integration of the four-wave system for another set of wave modes and for the time function of the diurnal cycle of the heat forcing being described by a half rectified sine. The modes considered in this integration are:

Mode 1: k1 = -2; n1 = -1 (Kelvin);

Mode 2: k2 = 5; n2 = 1 (Equatorial Rossby)

Mode 3: k3 = k1 + k2; l3 = 2 (barotropic mode);

Mode 4: k4 = -5; n4 = 3 (equatorial gravity);

As in Fig. 7, the results of the numerical integration of the four-wave system are displayed in Fig. 10 for different values of the parameter Q_0. However, the choice of the values of Q_0 is different from Fig. 7 because the selected modes are different, changing the necessary value of Q_0 to match the resonance condition. The results presented in Fig. 10 essentially

show the same qualitative features as those illustrated in Fig. 7. The initial conditions and the values of Q_0 to match the triad and duet resonances are different although the qualitative behavior is the same. This indicates that the choice between half wave rectified sine or fully rectified sine for the time dependent function of the convective heating does not affect the system in the timeframe of integration used in this work

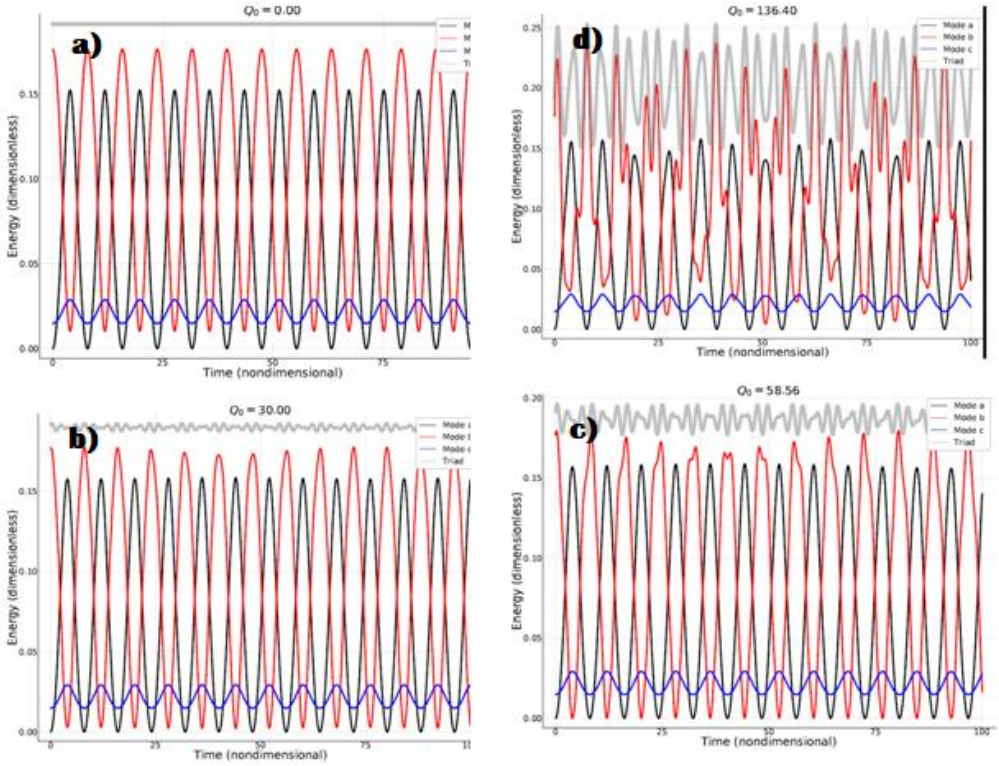

Figure 10: Similar to Fig. 7, but for another set of modes (see text) and for a diurnal cycle of the heat forcing being described by a half rectified sine function**.**

What this chapter has shown is that even with a simple theoretical framework it is possible to verify the complexity involved in understanding atmospheric dynamics and its evolution under global warming. Changing only the moisture content has shown to drastically alter the dynamics of the toy model. One can argue that the values displayed here are too small, however, it is plausible to think that inside an intense convection region the value of the moisture is greater than its climatological equilibrium value as well as the amplitude of the modes.

3 Chapter 4: CONCLUDING REMARKS

Here we have investigated the dynamics of a single triad interaction involving convectively coupled equatorial Rossby and Kelvin modes and a barotropic Rossby mode. The coupling between the equatorial wave modes and deep convection heating is described in the simplest possible setting by adopting the linear wave-cisk formulation in which the heating is proportional to the lower-troposphere moisture convergence produced by the waves, with the moisture field being prescribed to exhibit the meridional Kelvin mode structure, which is compatible with observations. If the diurnal cycle of the moisture field is considered, the triad is coupled with a fourth wave-mode, an equatorial inertia-gravity mode, through the linear wave interaction mechanism between equatorial Rossby and inertia-gravity modes proposed by Raupp and Silva Dias (2010). Overall, the results highlight two important effects of moisture. In the first one, the coupling between the equatorial Rossby and Kelvin wave modes with moist convection has shown to be a key feature to allow these equatorial wave types to undergo significant nonlinear triad interaction with the barotropic Rossby wave. In fact, the coupling with moisture reduces the eigenfrequencies of the equatorial wave modes, allowing the possibility of a barotropic Rossby wave to be resonantly coupled with the equatorial modes. Moreover, the results show that the moisture content can also influence the period of the energy modulations. Regarding the second effect, the coupling of the equatorial Rossby mode with the high frequency gravity mode through the diurnal cycle of the heat forcing also relies on the moisture content due to the effect of this parameter in controlling the frequency mismatch of this duet interaction. When this duo is coupled with the interacting triad through the equatorial Rossby mode, the moisture content also plays a relevant role in the dynamics of the four-wave system, since it can define which of the two resonances it gets the system closer to. In addition, when the gravity mode amplitude is high, which is compatible with an increased moisture content since gravity waves are closely related to deep convection, this coupling between the gravity mode with the interacting triad due to the moisture diurnal variation can significantly affect the triad interaction, with the energy being transferred back and forth

from the triad to the gravity mode. This can have an important implication to the nonlinear moist geostrophic adjustment problem.

As discussed in Chapter 1, convectively coupled equatorial Rossby and Kelvin modes play an important role in the morphology of the planetary-scale envelope associated with the MJO. In addition, the barotropic Rossby waves are believed to be the way by which the MJO affects the extratropics. Therefore, the reduced model of a single triad interaction involving these three wave types has been considered here as a toy model for the MJO activity, with the coupling with the high frequency equatorial gravity mode being a simple way to represent the effect of the high frequency convective systems embedded in the MJO. Consequently, the magnitude of the wave energy modulations in our toy model can be associated with the intensity of the MJO activity.

In this context, the increased wave amplitude modulations in our toy model in response to the moisture increase can suggest that increasing the moisture content of the atmosphere might lead to a stronger MJO activity. On the other hand, based on the Clausius-Clayperon equation, the higher the air temperature the higher the moisture content of the atmosphere.Consequently, one of the most direct effect of global warming is the increase in water vapor concentration in the troposphere. Therefore, the theoretical results presented here can provide a reasonable explanation for the observed increase of the MJO activity during last decades (Jones and Carvalho 2006), as well as its further increase foreseen to the remainder of this century in a scenario of pursued global warming (Jones and Carvalho 2011). Considering the MJO influence on extreme events of precipitation and temperature, the increase of its activity may help to explain changes in extreme values of these quantities associated with the increase of the global average temperature.

There is a large amount of uncertainty on how the MJO will respond to global warming, as well as the extreme climate events that are related to the MJO, such as heavy rainfall, and the changes in the hydrological cycle. In this scenario of great uncertainty, this work provides a direct and easily comprehensible mechanism bridging the gap between a direct response to a warmer planet and dynamical effects not easily simulated in GCMs used by IPCC projections.

Although we believe that this work has provided some important results and may help to shed some light into a possible mechanism underlying the change in climate variables in a warmer planet, there are some limitations in scope and applicability of the model adopted

here. First of all, it is not the intention of this work to be a comprehensive theory of the MJO, that is, a theory that accurately explains its whole structure and behavior, even though an important achievement of this work is that it helped understanding the dependency of the MJO on the mositure field in a dynamical framework. Second, even as a toy model, other important features are not considered here but are widely recognized as playing a key role in MJO system; one example is the heating associated with a shallow convection. The second baroclinic mode vertical structure needs to be included to represent the diabatic forcing associated with the shallow convection. Khouider et al. (2013) showed that the interaction between equatorial wave modes having the first and second baroclinic structures plays a significant role in the intraseasonal dynamics.

Another feature not considered here is the stochastic nature of the climate system. Several mathematical models use stochastic dynamics to reproduce the uncertainty that is inherently present in the nonlinear climate dynamics. One example is the effect of randomness of some variables or even a reduction of the dimension of the system where there are two or more distinct time and/or space scales involved (see, for instance, Majda et al., 2019 and Djikstra, 2013).

Finally, other limitation of the present work is the arbitrary nature of our choice of the dynamical system components. Other triads and interaction among triads should be considered in order to more accurately evaluate the evolution of the system.

Other limitations and critics could be pointed, however, it is our believe that, despite the simplicity of the model, its results provide interesting insights to further analysis and contribution to the climate change debate. Some suggestions to ameliorate the model accuracy are presented in the next chapter.

4 Chapter 5: FUTURE WORK AND SUGGESTION

Bearing in mind all the limitations of the model adopted in this work we proposed in this short chapter some studies necessary to improve our theoretical understanding of the MJO as a complex dynamical system.

a) To study the interaction of Equatorial Rossby mode with smaller scale gravity modes by considering a zonal structure of the diurnal cycle of convective heating that could help to understand the interaction between mesoscale gravity waves with large-scale Rossby waves. Also, the interaction of higher vertical modes of the system with the first baroclinic mode vertical structure associated with deep convection heating studied here, for instance, the interaction between first and second baroclinic modes. These interactions of the first baroclinic mode with higher vertical modes have shown to be important to accurately describe the whole MJO life cycle.

b) Applying the theoretical framework elaborated in this work to study the moist geostrophic adjustment processes.

c) To study the triad interaction with a forcing in one of its modes. This forcing could represent the projection onto the particular eigenmode of the radiative forcing associated with increased greenhouse gas concentration in the atmosphere. An important case that must be considered is the stratospheric cooling, which affects the gravest vertical modes in the troposphere.

d) To understand the effects of a forcing on the gravity mode on the triplet dynamics. Such forcing could mimic, for instance, the effect of global warming in enhancing deep convection activity, since gravity waves are the modes directly responsible for moist convection processes. This effect of enhancing convection by increasing the equilibrium value of the moisture content on the dynamics of our toy model has been analyzed here by artificially changing the gravity mode amplitude.

e) Using a stochastic forcing representing high frequency dynamics in the triad model to help to better understand how the variability of the MJO activity may change under global warming. For completeness, a study in this direction should use not only a white noise process but also a non-gaussian process.

f) An important feature missing in this work is the interaction with a more realistic basic state of the dynamical variables and the effect of the global warming over the basic state; for instance, a realistic atmospheric circulation pattern or a realistic spatial distribution of ocean surface temperature.

5 References:

ARNOLD, N. P., Z. KUANG, AND E. TZIPERMAN, 2013: Enhanced MJO-like variability at high SST. **J. Climate**, 26, 988–1001

BONY, S., STEVENS, B., FRIERSON, D. M. W., JAKOB, C., KAGEYAMA, M., PINCUS, R., SHEPHERD, T. G., SHERWOOD, S. C.,SIEBESMA, A. P., SOBEL, A. H., WATANABE, M. AND WEBB, M. J. (2015) Clouds, circulation and climate sensitivity. **Nature Geoscience**, 8 (4). pp. 261268.ISSN 17520894 doi:https://doi.org/10.1038/NGEO2398

BLACKMON, M. L.; Y. H. LEE; J. M. WALLACE. Horizontal structure of 500mb height fluctuations with long, intermediate and short time scales as deduced from lag-correlation statistics. **J. Atmos. Sci**, 41, 961-979, 1984.

BOYD, J. P. **Dynamics of equatorial ocean**. 1. ed. Berlin: Springer-Verlag GmbH Germany, 2018. 529 p.

BRETHERTON, C. S., M. E. PETERS, AND L. E. BACK, 2004: Relationships between water vapor path and precipitation over the tropical oceans**. J. Climate**, 17, 1517 1528,

BUI, H. X., AND E. D. MALONEY, 2018: Changes in Madden–Julian oscillation precipitation and wind variance under global warming. **Geophys. Res. Lett**., 45, 7148–7155, https://doi.org/ 10.1029/2018GL078504.

CARVALHO, L. M. V.; C. JONES; T. AMBRIZZI. Opposite phases of the Antarctic oscillation and relationships with intraseasonal to interannual activity in the tropics during the austral summer. **J. Climate**, 18, 702-718, 2005.

CHANG, C-P., H. LIM., 1988: Kelvin wave Cisk: A possible mechanism for the 30-50 day oscilations., **J.Atmos. Sci**, 45, 1709-1720;

CHEN, S., MAJDA, A. and STECHMANN, S. (2016). Tropical-Extratropical Interactions with the MJO Skeleton and Climatological Mean Flow. **Journal of the Atmospheric Sciences**. 73. 10.1175/JAS-D-16-0041.1.

COMPO GP, SARDESHMUKH PD. Removing ENSO-related variations from the climate record (vol 23, pg 1957, 2010). **J Clim 23**(22):6124–6127, 2010.

CRAIK, A. D. D. **Wave interactions and fluid flows**. Cambridge Monographs on Mechanics and Applied Math. Cambridge University Press., pp. 322, 1985

CUNNINGHAM CAC, CAVALCANTI IFA. Intraseasonal modes of variability affecting the South Atlantic Convergence Zone. Int J Climatol 26:1165–1180. 2006

DEMARIA, M. Linear response of a stratified tropical atmosphere to convective forcing. **J.Atmos. Sci**., 42(18), 1944-1959, 1985.

DIAS, JULIANA and PAULUIS, OLIVIER. Convectively Coupled Waves Propagating along an Equatorial ITCZ**. j atmos sci.** 66. 2237–2255 10.1175/2009JAS3020.1. 2009

DIJKSTRA, H. A. (2013), **Nonlinear Climate Dynamics**, pp. 367, Cambridge Univ. Press, Cambridge, U. K.

EASTERLING, D. R., J. L. EVANS, P. YA. GROISMAN, T. R. KARL, K. E. KUNKEL, AND P. AMBENJE, 2000: Observed variability and trends in extreme climate events: A brief review. **Bull. Amer. Meteor. Soc**., 81, 417–426

FLATO, G., J. MAROTZKE, B. ABIODUN, P. BRACONNOT, S.C. CHOU, W. COLLINS, P. COX, F. DRIOUECH, S. EMORI, V. EYRING, C. FOREST, P. GLECKLER, E. GUILYARDI, C. JAKOB, V. KATTSOV, C. REASON AND M. RUMMUKAINEN, 2013: **Evaluation of Climate Models. In: Climate Change 2013: The Physical Science Basis. Contribution of Working Group I to the Fifth Assessment Report of the Intergovernmental Panel on Climate Change** [Stocker, T.F., D. Qin, G.-K. Plattner, M. Tignor, S.K. Allen, J. Boschung, A. Nauels, Y. Xia, V. Bex and P.M. Midgley (eds.)]. Cambridge University Press, Cambridge, United Kingdom and New York, NY, USA.

FUCHS, N.; RAYMOND, D. J. A simple model of intraseasonal oscillations. **J. Adv. Modeling. Earth Sys.**, 9, 1195-1211, 2017.

GILL, A. E., 1980: Some simple solutions for heat-induced tropical circulation. **Quart. J. Roy. Meteor. Soc**., 106, 447–462,

GILL, A. E., 1982: Atmosphere–Ocean Dynamics. International Geophysics Series, Vol. 30, Academic Press, 662 pp

GRIMM, A. M. AND P. L. SILVA DIAS, 1995a: Use of barotropic models in the study of the extratropical response to tropical heat sources. J. Meteor. Soc. Japan, 73, 1037-1049;

GRIMM, A. M. AND P. L. SILVA DIAS, 1995b: Analysis of tropical-extratropicalinteractions with influence functions of a barotropic model. J. Atmos. Sci., 52 (20),3538-3555;

GRIMM, A.M. Madden–Julian Oscillation impacts on South American summer monsoon season: precipitation anomalies, extreme events, teleconnections, and role in the MJO cycle. **Clim Dyn** 53, 907–932 (2019). https://doi.org/10.1007/s00382-019-04622-6

HAYASHI, Y. A theory of large-scale equatorial waves generated by condensational heat and accelerating the zonal wind. **J. Meteor. Soc. Japan**, 48, 140-160, 1970.

HELD, I. M., AND B. J. SODEN, 2000: Water vapor feedback and global warming. **Annu. Rev. Energy Environ**., 25, 441–475

Holton, James R., An introduction to dynamic meteorology, Elsevier Academic Press,, Burlington, MA, pp. 535, 2004

HOREL, J. D.; J. M. WALLACE. Planetary-scale atmospheric phenomena associated with the Southern Oscillation. **Mon. Wea. Rev**.,109, 813-829, 1981.

HOSKINS, B.J.; D.J KAROLY. The steady linear response of a spherical atmosphere to thermal and orographic forcing.,J. Atmos. Sci., 38, 1179-1196, 1981.

HOSKINS., B. J.; A. J. SIMMONS; D. G. ANDREWS. Energy dispersions in a barotropic atmosphere**. Quart. J. R. Met. Soc.,** 103, 553-567, 1977

HOUZE, R. A., 2004: Mesoscale convective systems. **Rev. Geophys**., 42, G4003+

IPCC, 2013. Climate change 2013: the physical science basis. In: Stocker, T.F., Qin, D., Plattner, G.-K., Contribution of Working Group I to theFifth Assessment Report of the Inter- governmental Panel on Climate Change (AR5). Cambridge University Press, Cambridge, United Kingdom and New York, NY, USA .

IPCC, 2013. Summary for Policymakers. In Stocker, T. et al. (eds.) Climate Change 2013: The Physical Science Basis. Contribution of Working Group I to the Fifth Assessment Report of the Intergovernmental Panel on Climate Change, 1–29 (Cambridge University Press, Cambridge, United Kingdom and New York, NY, USA., 2013).

JIANG, XIANAN & WALISER, DUANE & XAVIER, PRINCE & PETCH, JON & KLINGAMAN, NICHOLAS & WOOLNOUGH, STEVEN & GUAN, BIN & BELLON, GILLES & CRUEGER, TRAUTE & DEMOTT, CHARLOTTE & HANNAY, CECILE & LIN, HAI & HU, WENTING & KIM, DAEHYUN & LAPPEN, CARALYN & LU, MONG-MING & MA, HSI-YEN & MIYAKAWA, TOMOKI & RIDOUT, JAMES & ZHU, HONGYAN. (2015). Vertical Structure and Physical Processes of the Madden-Julian Oscillation: Exploring Key Model Physics in Climate Simulations. **Journal of Geophysical Research**: Atmospheres. 120. n/a-n/a. 10.1002/2014JD022375.

JIANG, Z., S. B. FELDSTEIN, AND S. LEE, 2017: The relationship between the Madden–Julian Oscillation and the North Atlantic Oscillation. Quart**. J. Roy. Meteor. Soc.**, 143, 240–250

JONES, C. AND L. M. V. CARVALHO, 2006. Changes in the activity of the Madden-Julian oscillation during 1958-2004. **J. Climate**, 19, 6353-6370.

JONES, C. AND L. M. V. CARVALHO, 2011. Will global warming modify the activity of the Madden-Julian oscillation? **Quart. J. Royal Meteor. Soc**., 137 (655), 544-552

KHOUIDER, B., MAJDA, A. J., & STECHMANN, S. N. (2013). Climate science in the tropics: Waves, vortices and PDEs. **Nonlinearity,** *26*(1), R1-R68. [R1].

KILADIS, G. N., M. C. WHEELER, P. T. HAERTEL, K. H. STRAUB, AND P. E. ROUNDY, 2009: Convectively coupled equatorial waves. **Rev. Geophys**., 47, RG2003, doi:10.1029/2008RG000266

KNUTTI, RETO. (2008). Should we believe model predictions of future climate change? **Philos T R Soc A. Philosophical transactions. Series A, Mathematical, physical, and engineering sciences.** 366. 4647-64. 10.1098/rsta.2008.0169.

LAU, W. K.-M., AND D. E. WALISER, 2012: Intraseasonal Variability in the Atmosphere–Ocean Climate System. 2nd ed. Springer, 614 pp

LIEBMANN, B.; D. L. HARTMANN. An observational study of tropical-midlatitude interaction on intra-seasonal time-scales during winter. **J. Atmos. Sci**., 41, 3334-3350, 1984

LIN, H., G. BRUNET, AND J. DEROME, 2009: An observed connection between the North Atlantic Oscillation and the Madden–Julian oscillation. **J. Climate**, 22, 364–380

LINDZEN, R. S. 1974. Wave-CISK in the tropics. **J. Atmos. Sci**. 31, 156–179.

LE QUÉRÉ, C., PETERS, G. P., ANDRES, R. J., ANDREW, R. M., BODEN, T. A., CIAIS, P., FRIEDLINGSTEIN, P., HOUGHTON, R. A., MARLAND, G., MORIARTY, R., SITCH, S., TANS, P., ARNETH, A., ARVANITIS, A., BAKKER, D. C. E., BOPP, L., CANADELL, J. G., CHINI, L. P., DONEY, S. C., HARPER, A., HARRIS, I., HOUSE, J. I., JAIN, A. K., JONES, S. D., KATO, E., KEELING, R. F., KLEIN GOLDEWIJK, K., KÖRTZINGER, A., KOVEN, C., LEFÈVRE, N., MAIGNAN, F., OMAR, A., ONO, T., PARK, G.-H., PFEIL, B., POULTER, B., RAUPACH, M. R., REGNIER, P., RÖDENBECK, C., SAITO, S., SCHWINGER, J., SEGSCHNEIDER, J., STOCKER, B. D., TAKAHASHI, T., TILBROOK, B., VAN HEUVEN, S., VIOVY, N., WANNINKHOF, R., WILTSHIRE, A., AND ZAEHLE, S.: Global carbon budget 2013, **Earth Syst. Sci. Data**, 6, 235–263, https://doi.org/10.5194/essd-6-235-2014, 2014.

LYNCH, P., 2003: Resonant Rossby Wave Triads and the Swinging Spring. **Bull. Amer. Met. Soc**., 84, 605-616.

MADDEN, R. A., AND P. R. JULIAN, 1971: Detection of a 40–50 day oscillation in the zonal wind in the tropical Pacific. **J. Atmos. Sci**., 28, 702–708.

MADDEN, R. A., AND P. JULIAN, 1972: Description of a global-scale circulation cells in the tropics with a 40–50 day period. **J. Atmos. Sci**., 29, 1109–1123

MADDEN, R. A.; P. JULIAN. Observations of the 40-50 day tropical oscillation - A review. **Mon. Wea. Rev**., 122, 814-836, 1994.

MAJDA, A. ; SHEFTER, M.; Models for stratiform instability and convectively coupled waves, ***J. Atmos. Sci***., 58, 1567-1584, 2001

MAJDA, A. ; BIELLO, J. (2003). The Nonlinear Interaction of Barotropic and Equatorial Baroclinic Rossby Waves. Journal of The Atmospheric Sciences - **J ATMOS SCI**. 60. 1809-1821.

MAJDA, A.**. Introduction to PDEs and Waves for the Atmosphere and Ocean**, vol. 9 of Courant Lecture Notes in Mathematics, American Mathematical Society, Providence, 2003

MAJDA,A**.;** New Multiscale Models and Self-Similarity in Tropical Convection, J. **Atmos. Sci.**, Volume 64, Issue 4, April 2007, pp. 1393-1404

MAJ-
DA, A. J. AND S. N. STECHMANN, 2009: The skeleton of tropical intraseasonal osc illations. **Proc. Natl. Acad. Sci**., 106 (21), 8417.

MAJDA, A. J. et al. **Tropical Intraseasonal Variability and the Stochastic Skeleton Method**. 1. ed. New York: Springer Nature Switzerland AG, 2019. 131 p.

MAYTA, VC, AMBRIZZI, T, ESPINOZA, JC, SILVA DIAS, PL. The role of the Madden–Julian oscillation on the Amazon Basin intraseasonal rainfall variability. **Int J Climatol**. 2019; 39: 343– 360.

MATSUNO, T. Quasi-geostrophic motions in the equatorial area.**J. Meteor. Soc. Japan**, 44, 25-43, 1966.

MO, K. C.; R. W. HIGGINS. The Pacific-South American modes and tropical convection during the southern hemisphere winter. **Mon. Wea. Rev**., 126, 1581-1596, 1998.

MUZA, M.N., CARVALHO, L.M.V., JONES, C. AND LIEBMANN, B. (2009) Intraseasonal and Interannual Variability of Extreme Dry and Wet Events over Southeastern South America and the Subtropical Atlantic during Austral Summer. **Journal of Climate**, 22, 1682-1699.

MYHRE, G., ALTERSKJÆR, K., STJERN, C.W. et al. Frequency of extreme precipitation increases extensively with event rareness under global warming. Sci Rep 9, 16063 (2019).

MUZA, M. N.; CARVALHO, L. M. V. Variabilidade intra-sazonal e inter-anual de extremos na precipitação sobre o centro-sul da Amazônia. **Rev. Bras. Meteor**., 21, 29-41, 2006.

NEELIN, D. **Climate Change and Climate Modeling**. [S.l.]: Cambribge University Press, 2011. 300 p.

PEDLOSKY, J. **Geophysical Fluid Dynamics**. Springer Verlag, New York. 1987 710pp.

RAMIREZ, E.; SILVA DIAS, P. L.; RAUPP, C. F. M. Multiscale atmosphere-ocean interactions and the low-frequency variability in the equatorial region. J. Atmos. Sci., 74(8), 2503-2523, 2017.

SENEVIRATNE, S.I., N. NICHOLLS, D. EASTERLING, C.M. GOODESS, S. KANAE, J. KOSSIN, Y. LUO, J. MARENGO, K. MCINNES, M. RAHIMI, M. REICHSTEIN, A. SORTEBERG, C. VERA, AND X. ZHANG, 2012: Changes in climate extremes and their impacts on the natural physical environment. In: Managing the Risks of Extreme Events and Disasters to Advance Climate Change Adaptation [Field, C.B., V. Barros, T.F. Stocker, D. Qin, D.J. Dokken, K.L. Ebi, M.D. Mastrandrea, K.J. Mach, G.-K. Plattner, S.K. Allen, M. Tignor, and P.M. Midgley (eds.)]. A Special Report of Working Groups I and II of the Intergovernmental Panel on Climate Change (IPCC). Cambridge University Press, Cambridge, UK, and New York, NY, USA, pp. 109-230

STEVENS, D. E. AND LINDZEN, R. S. 1978. Tropical wave-CISK with a moisture budget and cumulus friction. **J. Atmos. Sci**. 35, 940–961

SIMMONS, A. J. The forcing of stationary wave motion by tropical diabatic heating. **Quart. J. R. Meteor. Soc**., 108, 503-534, 1982.

RAUPP, CARLOS & SILVA DIAS, PEDRO & TABAK, ESTEBAN & MILEWSKI, PAUL. (2008). Resonant Wave Interactions in the Equatorial Waveguide. **Journal of the Atmospheric Sciences**. 65. 3398-3418. 10.1175/2008JAS2387.1.

RAUPP, CARLOS & SILVA DIAS, PEDRO. (2009). Resonant Wave Interactions in the Presence of a Diurnally Varying Heat Source. **Journal of the Atmospheric Sciences**. 66. 3165-3183. 10.1175/2009JAS2899.1.

RAUPP, C. F. M. AND P. L. SILVA DIAS, 2010: Interaction of equatorial waves through resonance with the diurnal cycle of tropical heating. Tellus A, 62 (5), 706-718.

RAYMOND DJ (2001) A new model of the Madden–Julian oscillation. J Atmos Sci 58:2807–2819.

ROUNDY, P. E. Tropical–extratropical interactions. In: LAU, W. K. M.; WALISER, D. E. **Intraseasonal Variability in the Atmosphere–Ocean Climate System**. [S.l.]: Springer-Verlag Berlin Heidelberg, 2012. p. 648.

SILVA DIAS, P. L. , SHUBERT, W., H., 1983: Large-scale response of the Tropical Atmosphere to Transient Convection. **J. Atmos. Sci.**, 40, 2689-2707.

SOBEL, A., J. NILSSON, AND L. M. POLVANI, 2001: The weak temperature gradient approximation and balanced tropical moisture waves. **J. Atmos. Sci**., 58, 3650–3665.

SOLOMON, A., L. AND COAUTHORS, 2011: Distinguishing the roles of natural and anthropogenically forced decadal climate variability. **Bull. Amer. Meteor. Soc**., 92, 141–156

SOUZA EB, AMBRIZZI T (2006) Modulation of the Intraseasonal rainfall over Tropical Brazil by the Madden-Julian Oscillation. **Int J Climatol** 26:1759–1776

STAN, C., D. M. STRAUS, J. S. FREDERIKSEN, H. LIN, E. D. MALONEY, AND C. SCHUMACHER, 2017: Review of tropical–extratropical teleconnections on intraseasonal time scales. Rev. Geophys., 55, 902–937

VALLIS, G. K. Atmospheric and Oceanic Fluid Dynamics. Cambridge University Press, 2017.

WALLACE, J. M., AND D. S. GUTZLER, 1981: Teleconnections in the geopotential height field during the Northern Hemisphere winter. Mon. Wea. Rev., 109, 784–812.

WANG, B., AND H. RUI, 1990: Dynamics of the coupled moist Kelvin-Rossby wave on anequatorial □-plane., J. Atmos. Sci, 47, 397-413.

WANG, B., CHEN, G., LIU, F., 2019: Diversity of the Madden-Julian Oscillation. **Sci. Adv**. 5.

WANG, B. Theories. In: LAU, W. K. M.; WALISER, D. E. **Intraseasonal Variability in the Atmosphere–Ocean Climate System**. [S.l.]: Springer-Verlag Berlin Heidelberg, 2012. p. 648.

WANG, B., AND G. S. CHEN, 2016: A general theoretical framework for understanding essential dynamics of Madden–Julian oscillation. Climate Dyn., 49(7-8), 2309-2328, doi: 10.1007/s00382-016-3448-1

WANG,J., D. KIM, S. A. HENDERSON, C. STAN, AND E. D. MALONEY, 2019: MJO 739 teleconnections over the PNA region in climate models. Part I: Performance- and process-based skill metrics, J. Climate.

WHEELER, M. AND G. N. KILADIS, 1999: Convectively coupled equatorial waves: analysis of clouds and temperature in the wavenumber frequency domain. J. Atmos. Sci., 56 (3), 374399

ZEITLIN, V. **Geophysical Fluid Dynamics:** Understanding (Almost) Everything with Rotating. [S.l.]: Oxford University Press, 2018. 509 p.

ZHANG, C., 2005: Madden–Julian oscillation. Rev. Geophys., 43, RG2003,

ZHANG, C., 2013: Madden–Julian oscillation: Bridging weather and climate. Bull. Amer. Meteor. Soc., 94, 1849–1870